Protist, Vol. 157, 125—158, April 2006
http://www.elsevier.de/protis
Published online date 26 April 2006

Protist

Molecular Phylogeny of Cercomonadidae and Kinetid Patterns of *Cercomonas* and *Eocercomonas* gen. nov. (Cercomonadida, Cercozoa)

Serguei A. Karpov[a], David Bass[b], Alexander P. Mylnikov[c], and Thomas Cavalier-Smith[b,1]

[a]Department of Zoology, Herzen State Pedagogical University of Russia, Moika emb. 48, 191186, St. Petersburg, Russian Federation
[b]Department of Zoology, University of Oxford, South Parks Road, Oxford OX1 3PS, UK
[c]Institute for the Biology of Inland Waters RAS, Borok 152742, Russian Federation

Submitted February 28, 2005; Accepted January 24, 2006
Monitoring Editor: Michael Melkonian

Cercomonads are among the most abundant and widespread zooflagellates in soil and freshwater. We cultured 22 strains and report their complete 18S rRNA sequences and light microscopic morphology. Phylogenetic analysis of 51 *Cercomonas* rRNA genes shows in each previously identified major clade (A, B) two very robust, highly divergent, multi-species subclades (A1, A2; B1, B2). We studied kinetid ultrastructure of five clade A representatives by serial sections. All have two closely associated left ventral posterior microtubular roots, an anterior dorsal root, a microtubule-nucleating left anterior root, and a cone of microtubules passing to the nucleus. Anterior centrioles (= basal bodies, kinetosomes) of A1 have cartwheels; the posterior centriole does not, suggesting it is older, and implying flagellar transformation similar to other bikonts. Strain C-80 (subclade A2) differs greatly, having a dorsal posterior microtubule band, but lacking the A1-specific fibrillar striated root, nuclear extension to the centrioles, centriolar diaphragm, extrusomes; both mature centrioles lack cartwheels. For clade A2 we establish *Eocercomonas* gen. n., with type *Eocercomonas ramosa* sp. n., and for clade B1 *Paracercomonas* gen. n. (type *Paracercomonas marina* sp. n.). We establish *Paracercomonas ekelundi* sp. n. for culture SCCAP C1 and propose a *Cercomonas longicauda* neotype and *Cercomonas* (= *Neocercomonas*) *jutlandica* comb. n. and *Paracercomonas* (= *Cercomonas*) *metabolica* comb. n.

Keywords: centriolar transformation; *Cercomonas*; *Eocercomonas*; kinetid structure; *Paracercomonas*; 18S rRNA phylogeny.

Introduction

The recently established phylum Cercozoa (Cavalier-Smith 1998) has turned out to be one of the most morphologically diverse of all in the kingdom Protozoa (Cavalier-Smith and Chao 2003; Nikolaev et al. 2004; Polet et al. 2004) as well as one of the most speciose (Bass and Cavalier-Smith 2004). The classical genus *Cercomonas*

[1]Corresponding author.
e-mail tom.cavalier-smith@zoo.ox.ac.uk (T. Cavalier-Smith).

doi:10.1016/j.protis.2006.01.001

(Dujardin 1841) is the second most commonly and widely encountered zooflagellate genus in soil (Ekelund and Patterson 1997; Foissner 1991; Sandon 1927); they are also very common in freshwater (Arndt et al. 2000). Excluding the doubtful taxa of Skvortzov (1977), at least 49 *Cercomonas* species have been named (Mylnikov and Karpov 2004), but sequences of 18S rRNA genes amplified from environmental DNA extracts suggest that the real number is well over a hundred (Bass and Cavalier-Smith 2004). Moreover, the status of many — probably the majority — of the named species is uncertain, and the taxonomy of the genus urgently needs revision (Al-Qassab et al. 2002; Foissner 1991). Only a few species have been named from clonal cultures allowing proper appreciation of their range of variation and identification of cysts and plasmodial stages, if present (Mylnikov 1992c). Recently it became clear that there are two very distinct clades of *Cercomonas* on rRNA trees, which only sometimes group together as sisters (Bass and Cavalier-Smith 2004, Bass et al. 2005; Cavalier-Smith and Chao 2003).

A sounder *Cercomonas* taxonomy will come from integrated studies of numerous clonal cultures by light microscopy and DNA sequencing, and sampling a representative selection for thin-section electron microscopy. Accordingly we have isolated 21 new, mostly clonal *Cercomonas* cultures from freshwater and soil in Russia, Western Europe, Panama, and New Zealand, completely sequenced their 18S rRNA genes, and that of *C. longicauda* CCAP 1910/2, and carried out phylogenetic analysis to place them on the rapidly growing *Cercomonas* phylogenetic tree (51 sequences, including 10 additional previously unpublished sequences from environmental gene libraries to provide a more comprehensive tree). We also show phase contrast light micrographs of the general morphology of the cultured strains. Only a small number can be assigned to described species, but we shall give new names to most of those that cannot be identified thus only after studying still more strains.

Ekelund et al. (2004) recently confirmed the distinctiveness of *Cercomonas* clades A and B (their "type 1" is part of our clade B, and "type 2" part of clade A), described a new species *Neocercomonas jutlandica* within clade A, and applied the new generic name *Neocercomonas* to all "type 2" species. They introduced the useful idea of using signature sequences to improve cercomonad taxonomy, and distinguished *Neocercomonas* from *Cercomonas* solely by 18S rRNA signature sequences; however, as this was based on a very small database (7 sequences), their *Neocercomonas* signatures do not apply to all clade A, being absent from *C.* sp. E (Cavalier-Smith and Chao 2003). However, the culture designated as neotype for *Cercomonas longicauda* Dujardin (1841) by Ekelund et al. (2004) is not actually that species, and for this and other reasons is invalid as a neotype for it. Our present sequence signature analysis based on over 100 *Cercomonas* sequences and phylogenetic trees for 51 *Cercomonas* sequences clearly show that clade A is divisible into two major subclades, A1 (including *N. jutlandica*) and A2 (including *C.* sp. E), of which only clade A1 possesses the *Neocercomonas* signatures. As those cercomonads morphologically most resembling *C. longicauda* (Dujardin 1841), the type species of *Cercomonas*, are all in A1 and have the '*Neocercomonas*' signatures, *Neocercomonas* is probably a junior synonym of *Cercomonas* and thus is not adopted here. The early assumption that the classical genus *Cercomonas* is paraphyletic (Cavalier-Smith and Chao 1996/7) or polyphyletic (Ekelund et al. 2004) may be invalid, and a confusion caused by long-branch attraction artefacts (clade B having longer branches than clade A); in agreement with our earlier maximum likelihood analyses (Cavalier-Smith and Chao 2003) the best-sampled recent analyses consistently show classical *Cercomonas* as holophyletic by both distance and likelihood, albeit with weak support (Bass and Cavalier-Smith 2004; Bass et al. 2005).

Although there have been several ultrastructural studies of *Cercomonas* (Karpov 1997; Mignot and Brugerolle 1975; Mylnikov 1986b, c, 1987, 1989a, b, 1990, 1992a,b, 1995, 2000, 2002; Mylnikov and Mylnikova 2001; Mylnikov et al. 2000; Schuster and Pollack 1978), many were on unidentified species, none were of strains characterized by molecular phylogeny, and none used serial section reconstruction of flagellar roots, which is important for characterizing protist cytoskeletons, and of great phylogenetic significance (Karpov 2000a; Moestrup 2000). The fragmentary studies of cercozoan kinetids to date suggest a very considerable variation in flagellar roots among different major groups (reviewed briefly in Cavalier-Smith 2002). It is therefore possible that even though some *Cercomonas* strains that are genetically very distinct can look remarkably similar by light microscopy they differ internally quite substantially.

To test this we have serially sectioned and reconstructed kinetid ultrastructure of five phylogenetically diverse representatives of *Cercomonas* clade A, chosen from among those described

by light microscopy in this paper. This reveals common features of their cytoskeleton that only partially resemble those of the heteromitid *Katabia gromovi* (also order Cercomonadida and class Sarcomonadea), the only phagotrophic cercozoan previously with a detailed serial-section study of its kinetid ultrastructure (Karpov et al. 2003a), and probable synapomorphies for Sarcomonadea (cercomonads plus heteromitids). Furthermore, the most marked differences among clade A cytoskeletons are between those of subclades A1 and A2, indicating excellent correlation between kinetid and rRNA divergence. These and marked non-cytoskeletal ultrastructural differences between clades A1 and A2, plus their even sharper contrast with clade B, clearly justify three separate genera for the classical *Cercomonas*. Accordingly, we establish a new genus *Eocercomonas* for clade A2, and a new genus *Paracercomonas* for clade B1, and provide more definitive morphological and genetic signature diagnoses for *Cercomonas* sensu stricto. For brevity we use the term centriole throughout, rather than the synonyms basal body or kinetosome.

A striking new observation is that in *Cercomonas* sensu stricto (clade A1) the posterior centriole only lacks the cartwheel that is invariably present in the anterior centrioles. Since early developing centrioles have a central cartwheel as in other eukaryotes (Cavalier-Smith 1974), this shows that the posterior centriole is older than the anterior one and loses the cartwheel after assembly, providing the first evidence in Cercozoa, or any Rhizaria, for the typical bikont pattern of flagellar transformation (Cavalier-Smith 2002). In *Eocercomonas* (clade A2) neither mature centriole has cartwheels and in *Paracercomonas* (clade B1) both do.

Results

We first describe the molecular phylogeny to provide the evolutionary context for the microscopical data, enabling broad patterns to be discerned.

Phylogenetic Analysis

Figure 1 shows a Bayesian tree for 51 *Cercomonas* sequences; the 21 new strains and 10 new environmental sequences are spread widely across the tree, 24 in clade A and 7 in clade B. Two Russian strains (C-56 and C-72) are identical in sequence, but the other cultured strain sequences differ so substantially from each other and previous sequences that they are probably distinct species. Two other Russian strains cluster fairly closely together as a robust clade (C-59 and C-84), as do two Canadian environmental sequences (13-2.6 and 9-6.2) and two UK environmental sequences (10-3.6 and 8-3.1), all from different libraries. Apart from these, most clades contain strains from widely separate geographic locations. Within clade A there are two very divergent subclades, each with strong bootstrap support: A1, with 32 taxa and including *C. plasmodialis, C. longicauda* (CCAP 1910/2)*, C. (= N.) jutlandica* and *C. alexeieffi*; A2 comprises only five unidentified strains, for one of which we establish below a new species, *Eocercomonas ramosa*.

The speciose clade A1 itself comprises two distinct subclades (A1a, A1b). Although A1b lacks significant bootstrap support, it is supported by at least one unique signature (Table 1). Signatures identified for the A1b subclades (Table 1) strongly support the topology shown and indicate that *C. jutlandica* lacks close relatives among the present data set. The weak bootstrap support for clade A1b2, despite strong Bayesian support, is attributable to long-branch attraction pulling the very long branch of *Cercomonas* sp. 23 to the base of clade A1, an artifact to which Bayesian-likelihood methods seem more resistant. Apart from this, and a similar tendency for the lone *C. jutlandica* sequence to move towards the base of A1 in distance trees, there is excellent agreement between the distance and Bayesian analyses.

Clade B also consists of three major subclades (B1a, B1b and B2), all reproducibly holophyletic. Clade B1a is the most speciose, with 9 very distinct lineages and a fully resolved topology. Note that the two species that most resemble *C. cometa* in having highly branched filopodia are not mutually related: C-80 is in clade A2 and C-71 in clade B, showing that this morphotype is convergent. The two strains, Cs-4 and AZ-6, independently identified as *C. plasmodialis* are clearly not the same species, belonging to subclades A1a and A1b2 respectively; Cs-4 is actually the type strain (Mylnikov et al. 2000). *Paracercomonas* sp. 'small' (morphologically indistinguishable from Fig. 5 of Ekelund et al. 2004) is more closely related to *P. ekelundi* sp. n. (SCCAP C1, as '*Cercomonas longicauda*' sensu Ekelund et al. (2004); see discussion below) than to *P. marina* sp. n. (the new name proposed below for the ATCC 50344 culture also misidentified as *C. longicauda*). Most of the few differences (especially all the unique single nucleotide indels) between *P.* sp.

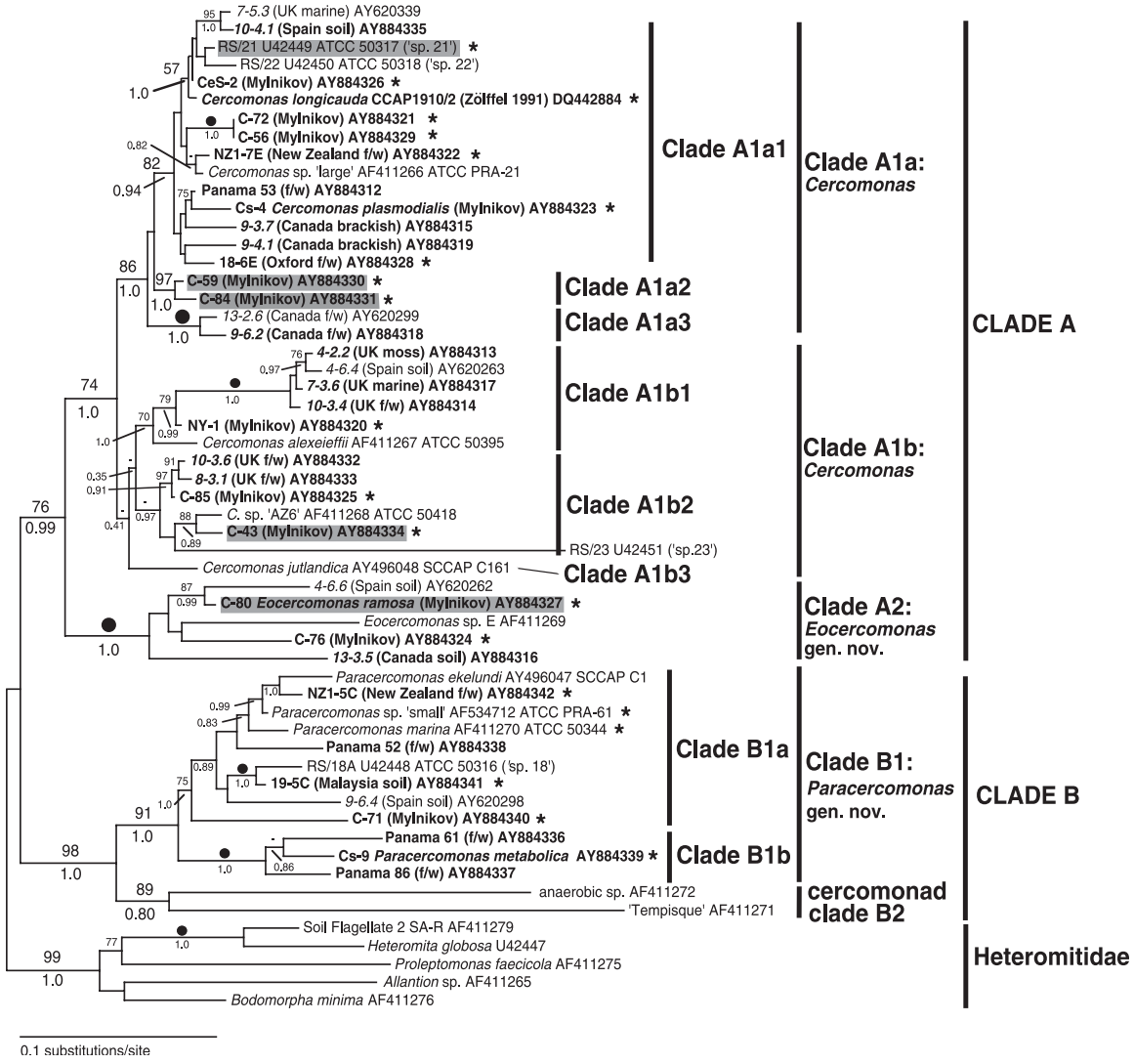

Figure 1. Consensus Bayesian likelihood tree for 51 Cercomonadidae sequences using 1013 nucleotide positions of the 18S rRNA gene, with Heteromitidae (Cercomonadida) as outgroup. A gamma intersite variation, covarion and autocorrelation GTR substitution model was used: see Methods for details. The figures and blobs at the nodes are distance tree bootstrap percentages for this dataset (upper) and Bayesian posterior probabilities (lower). All bootstrap percentages and posterior probabilities $\geqslant 75\%$ are shown; others lower than this are shown for clades of particular interest to this study. Black blobs indicate 100% bootstrap support. Dashes indicate nodes for clades not found in the consensus distance tree. Italicized numerical codes refer to sequences obtained from Cercozoa-specific environmental gene libraries. The strains whose ultrastructure is described here are shaded in grey; asterisks indicate strains illustrated in Figures 3 and 4. The 32 new sequences are shown in bold. f/w = fresh water.

small and *P. ekelundi* (SCCAP C1) could be sequencing errors; some of those that distinguish *P. marina* (‘*Cercomonas longicauda*’ ATCC 50344) from *P. ekelundi* (SCCAP C1) are genuine, having been confirmed by two independent laboratories (Cavalier-Smith and Chao 2003), but others are more doubtful and probably sequencing errors (mainly in the AF101052 sequence). However, the fact that these two distinct sequences each formerly identified as *longicauda* are in clade B1, whereas the CCAP *longicauda* is in clade A1 means that they are not all the same species, and at least two were misidentified. As the CCAP *longicauda* is morphologically markedly closer to

Table 1. 18S rDNA sequence signatures for clades of *Cercomonas*, *Eocercomonas*, and *Paracercomonas* as indicated on Figures 1 and 2.

Clade code[1]	Sequence signature (bold)[2]	Position[3]	Notes[4]
A1	**CA**GCTCATTAAATCAGT**C**AT**T**	96/H8, ~V2	a
A1	GAGGGACTATCGGT$_C$G***A***TTTA	1402, H44	b
A1	TCGAGC$_T$TTACAACCTTG**G$_T$T$_C$T**	1504, H46	c
A1	**GGACT**	859	
A2	T**A**AT**T**	112/H8, ~V2	d
A2	TCGAGC$_T$TTACAACCT**TGACT**	1504, H46	
A2	CTT$_C$**CTGTTC**TATTTTGTTGGTTTCTAGGA**T$_C$GG**	833, E23_13/14, V4	
A1a	C**A$_{C/T}$T**CCATCCTTCG	700/HE23_1, V4	
A1b	**CTC$_T$AG**	498/H17, V3	
A1b1	GC**TTCGG**	666	e
A1b1	TCT-CCCTTC$_T$AT$_C$TGGGTTGG$_A$G**CCGGA**	723, E23	f
A1b2	G$_A$CCATCC**A**	702, E23_1, V4	g
B1	**T**CGGCCAGAGGTGAAATTC$_T$TTGGATTCG**A**	907, H25	h
B1	T**T**AT**AG**	112/H8, ~V2	

[1]As indicated on Figure 1.
[2]Bold nucleotides = ancestral synapomorphy for clade (where >1 nt marked, that particular combination is unique to the clade: within Cercomonadidae, unless otherwise stated. Subscript nucleotides = rare secondary changes to the preceding nucleotide.
[3]Helix (H, E) and variable region (V) location according to Wuyts et al. (2000) / position of LH-most nucleotide of signature sequence relative to *Cercomonas* sp. 'Large' (AF411266 ATCC PRA-21).
[4]**Notes:**
[a]cf. signatures for clades A2 and B at same position.
[b] = signature sequence N1 in Ekelund et al. (2004). Insertion of ***A*** (pos. 1417) is a synapomorphy for clade A1, once changed to C (in 19-3E).
[c] = signature sequence N2 in Ekelund et al. (2004) to define *Neocercomonas*. Possible confusion/convergence with clade B. Three positions are variable and converge with B, but this signature clearly distinguishes clade A1 from A2.
[d]cf. signatures for clades A1 and B at same position.
[e]Unique within Cercozoa.
[f]'—' indicates a shared deletion in this clade.
[g]Unique within Cercozoa.
[h]Highlighted nucleotides show compensatory base change synapomorphy for clade B1 secondarily reversed in Cs-9.

Dujardin's (1841), as explained below, both the ATCC and the SCCAP strains were misidentified, and we describe them below as new species in a new genus *Paracercomonas*.

Sequence Signature Analysis

Sequence signatures that are distinctive for particular subclades of cercomonads were sought by visual examination of a large alignment of over 100 cercomonad sequences and a representative selection of other Cercozoa; the signatures shown in Table 1 are not necessarily unique to cercomonads, as a complete eukaryote alignment was not studied, but all unambiguously differentiate the specified subclades from all other cercomonads in our database, and in some cases also from all other Cercozoa, as noted in Table 1. Sequence signature analysis strongly supports the major split between clades A1 and A2, with four clear synapomorphies for each. However, N2 of Ekelund et al. (2004) does not discriminate between clade A1 and all clade B sequences in our database, as several clade B sequences have convergent substitutions. Thus only the first three A1 signatures are taxonomically diagnostic for clade A1. All the sequence signatures in Table 1 were checked for consistency with over 50 additional complete unpublished *Cercomonas* sequences in our database (Bass and Cavalier-Smith) — over 100 sequences altogether. Fig. 2 shows a comparative alignment of the regions surrounding some of the more important signatures.

None of the four sequences suggested by Ekelund et al. (2004) to be diagnostic for their type 1 *Cercomonas* (our *Paracercomonas*, see below) is diagnostic for the whole of clade B. The second A in their C1 is a synapomorphy only for clade B1, as our '*Cercomonas'* Tempisque and '*Cercomonas'* sp. 'anaerobic' sequences (Cavalier-Smith and Chao 2003) previously indicated. That mutation of a C to an A is invariably accompanied by a G—T substitution 28 nucleotides earlier in the sequence and is clearly a conserved and derived complementary base-pair substitution that uniquely defines clade B1, except for two known reversions, e.g. in Cs-9; secondary structure alignments show that these two nucleotides are indeed a derived U—A base pair (base pair 7 in helix 25) compared with the ancestral state (G—C) for Filosa. The first G and last T in their C4 (Ekelund et al. 2004) is a synapomorphy not for clade B, but for clade B1 only. Their C2 is not diagnostic for clade B, as it is too variable within the clade; our database shows mutations at nine positions. The position of the third T could be diagnostic, as it is always a T, C or A in clade B and always a G in clade A, but its variability would make that choice risky. Their C3 is also far too

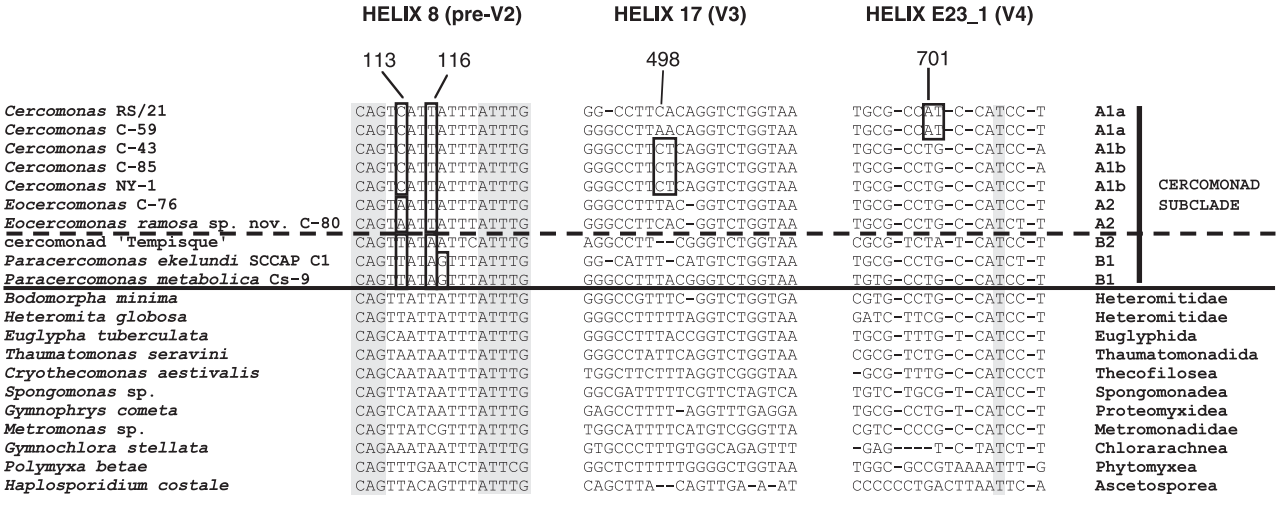

Figure 2. Comparative alignment of the regions surrounding some of the more important sequence signatures. Shaded regions indicate positions conserved across Cercozoa. Boxes indicate clade-specific diagnostic signatures and their position relative to the sequence of *Cercomonas* sp. 'Large' (AF411266 ATCC PRA-21), which are also shown on Table 1; helix (H, E) and variable region (V) location according to Wuyts et al. (2000) are also shown for each alignment region. The dashed and solid horizontal lines mark the boundaries between Clade A, Clade B, and other Cercozoa.

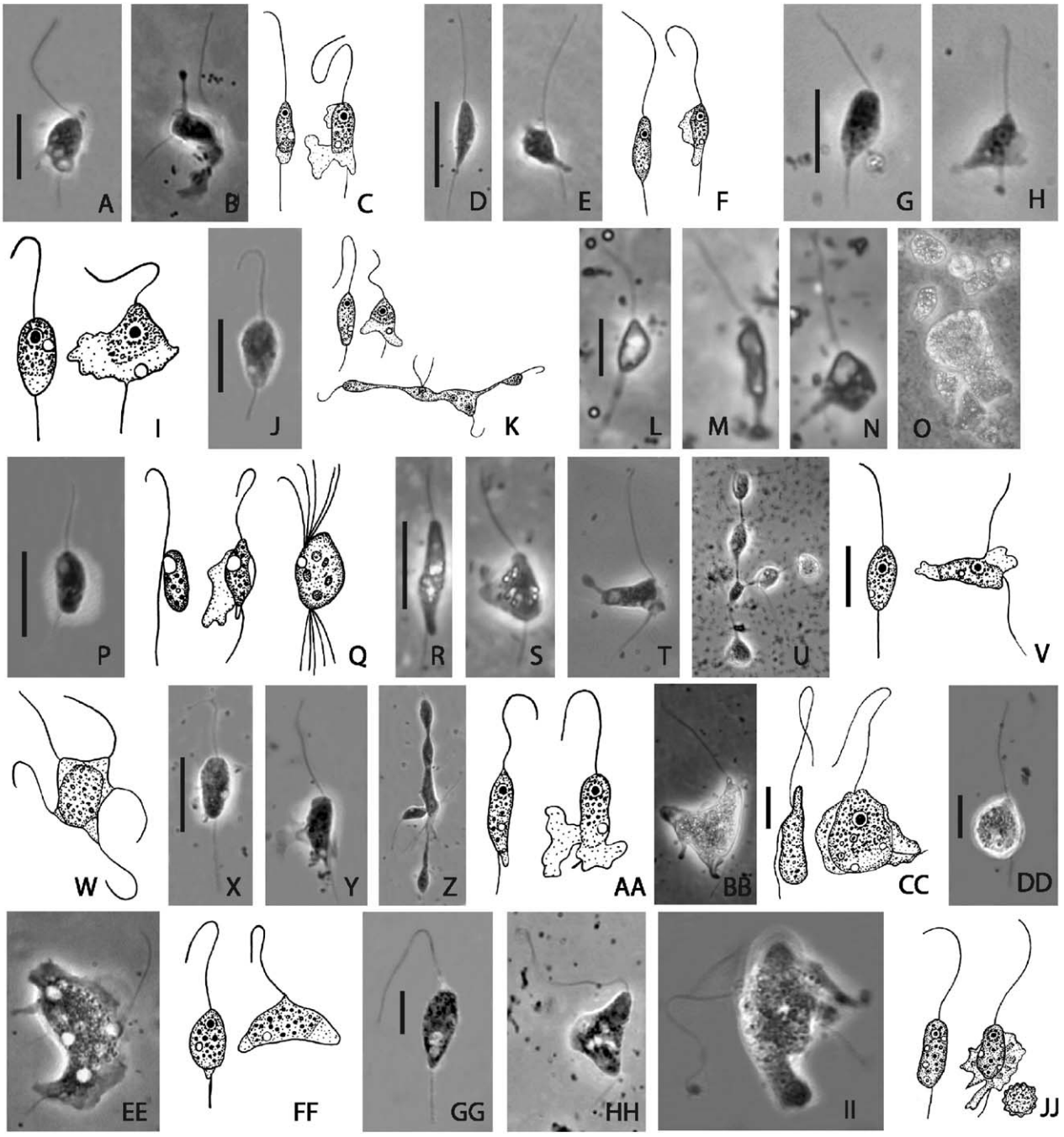

Figure 3. Photomicrographs and drawings of selected *Cercomonas* strains. Scale bars representing 10 μm are given for the flagellate stages only (the most reliable and reproducible stage to measure). *Abbreviations*: am = amoeboid form; am/flag = amoebo-flagellate form; draw = interpretive drawing; flag = flagellate form; plas = plasmodial form.
Clade A1a: A—C: **strain RS/21** flag-am-draw; D—F: **strain CeS-2** flag-am-draw; G-I: **strain C-72** flag-am-draw; J—K: **strain C-56** flag-draw (incl. plas); L-O: **strain NZ1-7E** flag-am/flag-am-plas; P—Q: **strain Cs-4** flag-draw (incl. plas); R-S: **strain 18-6E** flag-am; T-W: **strain C-59** am-plas-draw-plas; X—AA: **strain C-84** flag-am-plas-draw; **clade A1b1:** BB—CC: **strain NY-1** am-draw; **clade A1b2:** DD—FF: **strain C-85** flag-am-draw; GG—JJ: **strain C-43** flag-am-plas-draw.

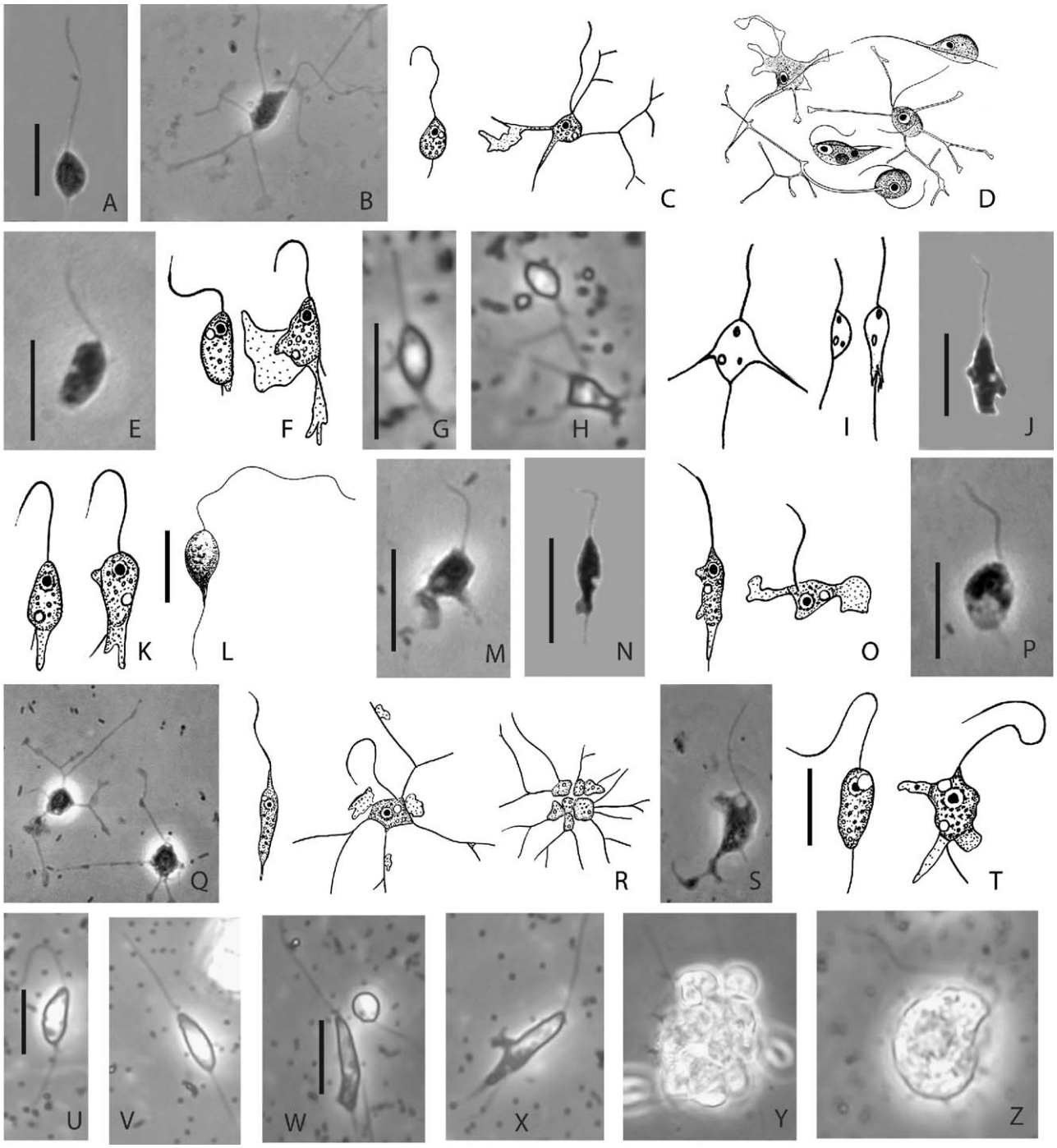

Figure 4. Photomicrographs and drawings of selected cercomonad strains. 10 μm scale bars are given for flagellate stages only. *Abbreviations*: am = amoeboid form; am/flag = amoebo-flagellate form; draw = interpretive drawing; flag = flagellate form; plas = plasmodial form.
Clade A2. (*Eocercomonas*): A—D: ***Eocercomonas ramosa* (strain C-80)** flag-am-draw (Mylnikov)-draw (Hollande 1942); E—F: **strain C-76** flag-draw; **clade B (*Paracercomonas*) and *C. longicauda*:** G—I: **strain NZ1-5C** flag-am-draw; J—K: ***Paracercomonas marina* ATCC 50344 '*longicauda*'** am/flag-draw; L: ***C. longicauda*** scanned from Dujardin (1841); M: ***C.* sp. 'small' strain PRA-61** am/flag; N—O: **strain 19—5C** am/flag-draw; P—R: **strain C—71** flag-am-draw; S—T: ***Paracercomonas metabolica* comb. nov. Cavalier-Smith and Bass strain Cs-9** am/flag-draw. U—Z: ***Cercomonas longicauda* neotype CCAP 1910/2** - U,V flag-W,X am/flag - Y cell cluster - Z plas.

variable, 16 of the nucleotide positions varying within clade B, and under half our clade B sequences sharing C3. Thus of their signatures for *Cercomonas* sensu Ekelund et al. (2004) would delimit clade B1, whereas the other two would define a broader group; thus C1-C4 are not suitable collectively for defining any genus. The signature sequence that Ekelund et al. (2004) used to define *Cercomonas 'longicauda'* (our *P. ekelundi*) is not totally specific for their strain, but would identify six very closely related ribotypes in our database (including *Cercomonas* sp. small; its 4 unique single-nucleotide indels and one in their strain sequence are probably sequencing errors) differing in very few nucleotides elsewhere in the molecule (sometimes just one).

Light Microscope Morphology

Figure 3 shows phase contrast micrographs and drawings of the strains at different stages of the life cycle of a broad sample of 12 clade A1 strains (*Cercomonas* sensu stricto) arranged in the order on the tree (Fig. 1). It is immediately obvious that subclade A1a cells are on average smaller than A1b cells: mostly under 10 μm long, whereas clade A1b cells are mostly over 10 μm and have particularly long flagella. *Cercomonas jutlandica*, the sole representative of clade A1b3, is also large (10—16 μm) (Ekelund et al. 2004) and most closely resembles C-85 from clade A1b2 (Figs 3 DD—FF). Of the four strains first studied phylogenetically (Cavalier-Smith and Chao 1996/7), sp. 23 (clade A1b2) was markedly larger than species 21 and 22 (clade A1a1) or 18 (clade B). Figure 4 similarly illustrates two clade A2 and six clade B strains; most are similar in size to those of clade A1a. This surprising correlation between cell size and large-scale phylogeny needs further testing, but it appears that cercomonads were ancestrally small and that cell size increased in the common ancestor of clade A1b; this increase may be significant in relation to the marked ultrastructural differences in cytoskeleton between clades A1 and A2 reported below.

Inspection of Figure 3 also shows that pseudopods of all clade A1 strains are broad lamellipodia, never branched filopodia. However, although some members of clades A2 and B produce similar broad pseudopods, others have simple or branched filopodia. C-80 in clade A2 and C-71 in clade B produce very similar highly branched pseudopodia; initially both were misidentified as *Cercobodo cometa*, but differences in flagella dimensions indicate that neither is really *C. cometa*. Clearly their branched filopodia evolved independently; there must be at least three different species of cercomonads with *cometa*-like morphology, so great care is needed in future identification. Both strains constituting subclade A1a2 (C-59 and C-84) are very prone to form linear chains of incompletely divided cells (Figs 3 U,Z). This behaviour is rarer in clade A1a1, being noted only in C-56 (Fig. 3 K). It is significant that all A1a1 strains are very similar morphologically; yet small differences can be seen, even between the two strains with identical 18S rDNA sequences (C-72 and C-56), making it likely that all 51 strains shown in Figure 1 are different species.

The classical distinction between *Cercobodo* (flagella separate from cell, e.g. NY-1 of clade A1b1 and Cs-4 of clade A1a1) and *Cercomonas* (flagella strongly adhering all along the length of the cell, e.g. C-43 of A1b2) (Krassilstschik 1886) is not of deep phylogenetic significance, but can be a very reliable character for discriminating certain strains. Contractile vacuoles are generally present and occur at specific places in motile cells of each strain. Note that *P. marina* (ATCC '*C. longicauda'*) (Figs 4 J,K) is not markedly different in morphology from the closely related, but ribotypically distinct *P. ekelundi* ('C. *longicauda'* of Ekelund et al. 2004); judging from their figs 5 and 12 (not clearly stated in their description), their strain may have a greater tendency for the posterior flagellum to adhere to the trailing cytoplasm. Our *Paracercomonas* 'small' is closely related to and morphologically very similar to both. Descriptions are given below of the five clade A strains selected for ultrastructural study.

Cercomonas strain C-84 (Figs 3 X—AA)

Cells are ovoid or spindle shaped, 8.3—11.6 μm long. Both flagella are 1.5—2 times longer than the cell. Contractile vacuole is in the posterior part of the cell. Small plasmodia are about 25 μm in diameter. Cysts not found.

Cercomonas strain C-59 (Figs 3 T—W)

Spindle-shaped body with pointed posterior end, 9.9—13.2 μm in length. Anterior flagellum 1.5—2 times, and posterior 2—3 times longer than body. Contractile vacuole is in the posterior part of the cell. Pseudopodia flat and broad. May produce plasmodia. Cysts 5—6.6 μm in diameter.

Cercomonas strain RS/21 (ATCC 50317: *Cercomonas* sp. 21 of Cavalier-Smith and Chao 1996/7: Figs 3 A—C)

Moving cells are oval, 8—14 μm long, anterior flagellum is 2—2.5 longer and the posterior is 1.5—2 times longer than the cell body. One, rarely two, contractile vacuoles lie at the anterior part of the cell near the nucleus. Unbranched lamellate pseudopodia form at the posterior or middle part of the cell. Cyst diameter 5—8 μm.

Cercomonas strain C-43 (Figs 3 GG—JJ)

The cell body has a broad-oval shape; markedly metabolic. There are one or two tail pseudopodia, it can also produce short lateral ones. Cell length is normally 15—20 μm; equal flagella a bit longer than the body. Recurrent flagellum applies to the cell, even if it turns or overcomes obstacles. One or two contractile vacuoles at the cell posterior. This strain was studied ultrastructurally as *C. crassicauda* by Mylnikov (1989a), but as it is much larger than *crassicauda* of Dujardin (1841; 6—10 μm) and has an obviously projecting posterior flagellum not usually obscured by a cytoplasmic tail, it was probably misidentified. Note that strain RS18A, which is in clade B1a, unlike C-43, was labeled *C. crassicauda* by Cavalier-Smith and Chao (1986/7) following tentative identification by Humphrey Smith (Coventry), but that may not be correct either and the true identity of *C. crassicauda* requires clarification. Cysts 9—15 μm; surface rough or wavy with blunt angular protuberances.

Eocercomonas ramosa sp. nov. strain C-80 (Figs 4 A—D)

Moving cells are spindle shaped, 5—15 μm long. Proximal part of anterior flagellum is surrounded by a cytoplasmic sheath. Posterior flagellum is almost invisible. Contractile vacuole is in the anterior part of the cell. Trophic cells produce highly branched filopodia, and may group together forming consortia. Cysts infrequent; smooth, spherical; c. 5 μm.

Almost identical to C-71, but has much longer anterior flagellum. Cysts not recorded in C-71. C-80 and C-71 are similar to *Cercobodo cometa* Hollande (1942), but differ in both having relatively much shorter posterior flagella.

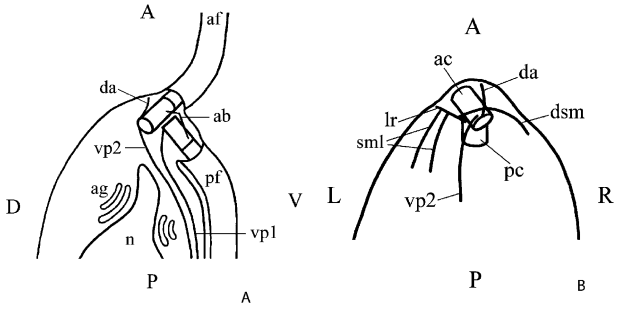

Figure 5. Kinetid orientation and flagellar roots of *Cercomonas* (clade A1). The direction of some of the roots is shown. **A:** View from the right side of the cell. **B:** View from the dorsal side of the cell. A — Anterior, P — Posterior ends; D — Dorsal, V — Ventral, L — Left, R — Right sides of the cell. As the discussion explains, the anterior centriole is younger and the posterior one older; thus flagellum 1 is posterior and flagellum 2 anterior, according to recent convention (Moestrup 2000), and we label the ventral posterior roots vp1 and vp2, according to their respective attachments to posterior centriole 1 and anterior centriole 2.

Abbreviations for Figures 5—14: ab — anterior fibrillar bridge, ac — centriole (basal body, kinetosome) of anterior flagellum, af — anterior flagellum, ag — Golgi apparatus, c — centriole (basal body, kinetosome), cf — concentric fibre (rings), cs — centrioles (basal bodies), cv — contractile vacuole, da — dorsal anterior root, di — diaphragm structure, dp — dorsal posterior root, dsm — dorsal band of secondary microtubules, er — endoplasmic reticulum, fb — fibrillar bridges connecting centrioles and centrioles with roots, ff — fibrillar foot, fr—fibrillar root, fsr — fibrillar striated root, lr — left anterior root, m — mitochondrion, mb — microbody, mc — microtubular cone, mr—microtubular root, mrb — mushroom-like bodies, mtc—microtoxicysts, n — nucleus, nu — nucleolus, ob—osmiophilic bodies, og — osmiophilic granule, om — osmiophilic material, pc—centriole of posterior flagellum, pf — posterior flagellum, pp — proximal partition of pc, pr — fibrillar projection from pc, ps — pseudopodium, sb — symbiotic bacteria, sm—secondary microtubules, sma—pair of microtubules from anterior centriole, sml — secondary microtubules from left root, vp — ventral posterior roots, vp1 — ventral posterior root of posterior flagellum, vp2 — ventral posterior root of anterior flagellum.

Electron Microscopy

Kinetid pattern and general ultrastructure of five cercomonad strains were investigated: C-84, RS/21, C-43, C-59 from clade A1 (*Cercomonas*) and

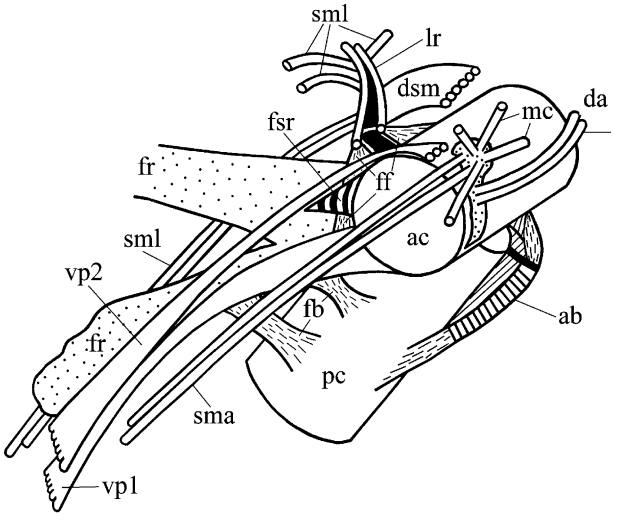

Figure 6. Reconstruction of kinetid structure of *Cercomonas* strain C-84 (clade A1). Viewed from above (dorsal side) but from the right (i.e. at an angle intermediate between Figs 5 A and B; for abbreviations see Fig. 5 legend). To display the roots more clearly in this perspective drawing and for ease of comparison with strain C-80 (Fig. 14) the apical angle between the centrioles has been altered from the correct 90° to make it more obtuse than it is in this strain.

C-80 from clade A2 (*Eocercomonas ramosa*). All strains studied differ in details of flagellar apparatus and general ultrastructure. General ultrastructural features of C-43 (as *Cercomonas 'crassicauda'*) investigated earlier (Mylnikov 1989) were confirmed. Although four other strains (C-84, RS/21, C-59 and C-80) were investigated for the first time, we focus mainly on their kinetid structure, which is complex and substantially different from that of all other protists. To orient the reader we outline common features before describing each strain in detail.

Both flagella insert at the cell apex and are mutually attached by their centrioles (shown schematically in Figs 5 A,B). Flagella are smooth, lacking paraxonemal structures. The anterior flagellum points slightly to the left of the central line and often beats asymmetrically to the left. Both centrioles lie almost in one plane. The centriole of the anterior flagellum typically points forward and to the left; the base of the posterior centriole is attached to the middle part of the ventral side of the anterior centriole at an angle of 90° or more, and its flagellum bends back to run along the mid line of the cell. It usually lies in a groove or channel, depending on the species, but in some may be less closely attached to the cell. At least three fibrillar bridges interconnect the centrioles. The anterior fibrillar bridge is best developed (Fig. 5 A). The centriole of the posterior flagellum has much more prominent fibrillar matrix around it than the anterior one.

Two prominent ventral posterior roots of several microtubules are always associated with the centrioles, one (VP2) stemming from the anterior and one (VP1) from the posterior centriole. They probably provide mechanical support for the ventral groove/channel when it is present (C-80, C-43). As the cells are too large for economically serially reconstructing the entire cytoskeleton, this paper concentrates on flagellar transition zones, centrioles, and nearby cytoskeletal structures, which include many dense fibres and a variety of microtubular roots (summarized in Fig. 6 for clade A1). In all strains the nucleus is subtended by a microtubular cone emanating from a nucleating centre associated with the centrioles, but its nature and the geometry of association vary. As explained in the discussion, ultrastructural differences among the strains correlate well with the molecular tree. Those of the four clade A1 strains (C-84, RS/21, C43, C-59) are broadly similar and described first, whereas C-80 (clade A2) differs in important respects. We describe C-84 in detail; the other species are more briefly compared with it.

Cercomonas strain C-84 (Figs 6—8)

General ultrastructure. Both flagella emerge from an apical tapering (Fig. 7 A). The vesicular nucleus has a large central nucleolus and prominent anterior projection directed towards the centrioles. One or two Golgi dictyosomes attach to one or both sides of this nuclear projection. Mitochondria predominantly have slightly flattened tubular cristae, not vesicular or typical tubular ones (Figs 7 A,B, 8 F). Microbodies are partly applied to the nucleus and partly located in the posterior cytoplasm. Extrusomes are rare, simple osmiophilic bodies, normally under the plasma membrane of the anterior half of the cell. There are many large membrane-bounded bodies with central masses of dense material surrounded by numerous black dots or curved rods, which resemble the mushroom-like bodies (MRBs) of *Katabia* (Karpov et al. 2003a) but differ in lacking an internal stalk and crystal-like structure. The cytoplasm is filled with rough endoplasmic reticulum (ER) cisternae, ribosomes, and vesicles of

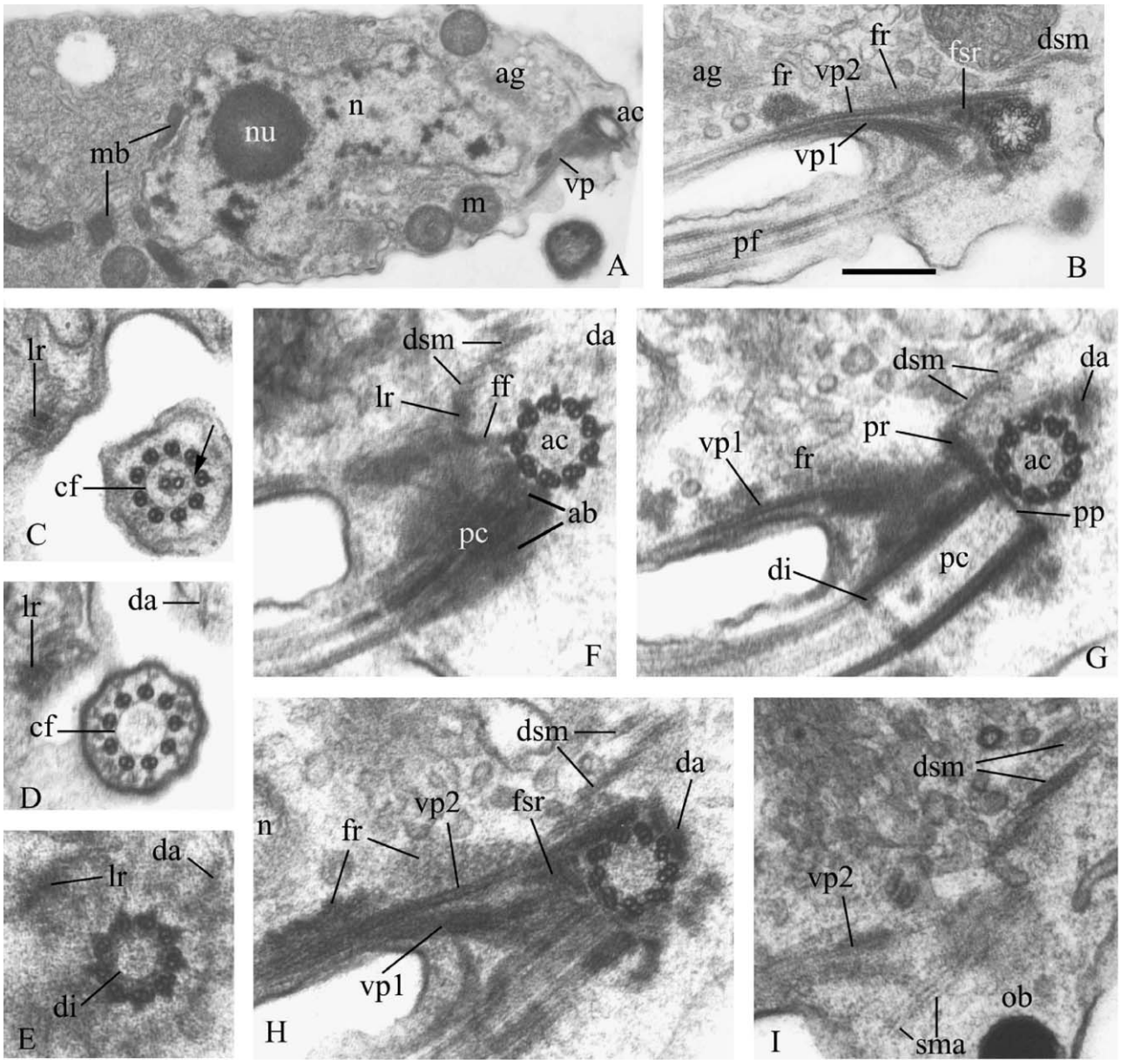

Figure 7. General view and kinetid structure of *Cercomonas* strain C-84. **A:** General view of the cell in saggittal section. **B:** The kinetid sectioned through anterior centriole base (viewed from base to tip of anterior flagellum) showing the divergent bases of the ventral posterior roots (vp1,2). **C—I:** Selected consecutive cross-sections of the anterior centriole from the axoneme to its base (viewed from base to tip of anterior flagellum). **C:** Axoneme: arrow shows a partition between A and B tubules, to which a concentric fibres (cf) attaches. **D:** Transitional zone with concentric fibres (cf). **E:** Distal end of centriole showing diaphragm-like periphery (di) of the distal partition. **F—H:** Longitudinal sections of posterior centriole. **I:** Section just beneath and slightly grazing the anterior centriole. Scale bar: A — 1 μm; B — 300 nm; C—I — 200 nm.

different size. The posterior flagellum lies in a groove supported by microtubules.

Flagellar apparatus. The transition zone of both flagella is very short; in transverse sections a very slender ring (cf; or concentric rings, using the terminology of Andersen et al. 1991) is visible, connected to a short projection from the junction between the axonemal A- and B-tubules (Figs 7 C,D). Both centrioles have a thick plate

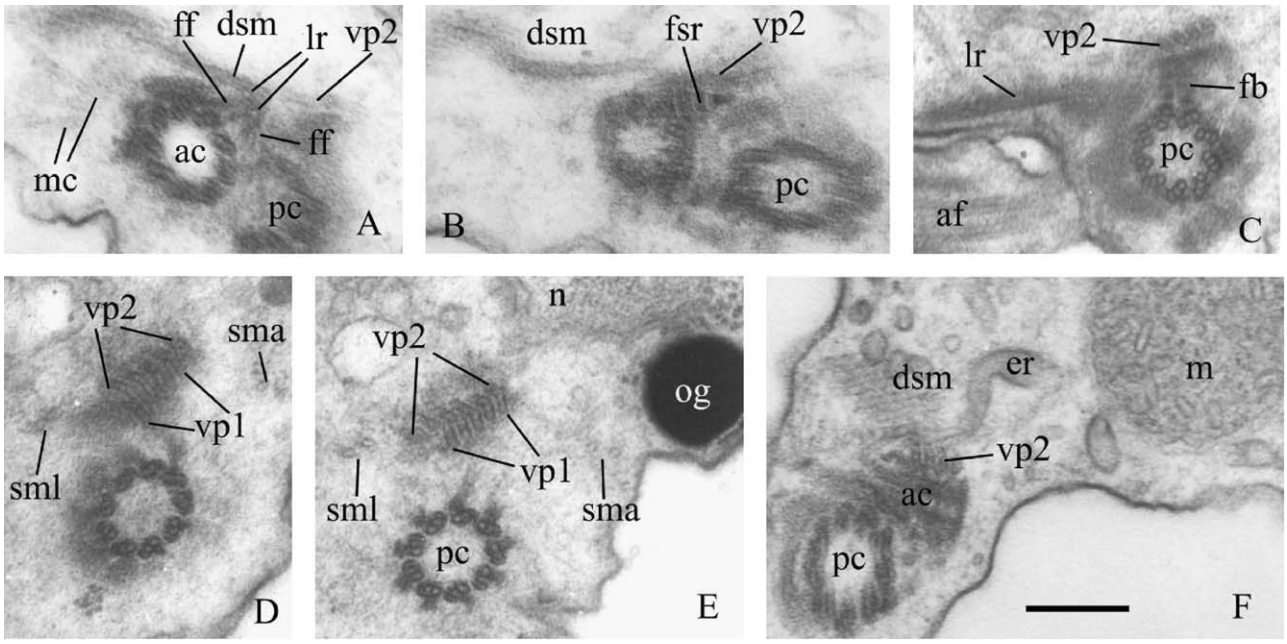

Figure 8. Kinetid structure of *Cercomonas* strain C-84. **A—B:** Consecutive sections of anterior centriole from tip to base (viewed from tip to base) to show the origin of left anterior root (lr). **C—E:** Series of consecutive cross-sections of the posterior centriole (viewed from tip to base), showing the ventral posterior roots and the origin of root vp1. **F:** Section through the apical end of the cell showing the origin of vp2, and cristae structure of mitochondrion. Scale bar: A—F — 200 nm.

across the distal end — the distal partition (di; its central region is of medium density but its periphery is a much denser ring resembling a partially open diaphragm (Fig. 7 E). There is a marked differentiation between the lumenal structures of the two centrioles. The anterior one (ac) has the usual cartwheel proximally, extending about a quarter of its length, and the upper part of its lumen is fairly homogeneously fibrous (Figs 7 B,G). The posterior centriole (pc) only is sealed at its very base by a dense transverse plate — the proximal partition (pp); it lacks a cartwheel and the lumen is less homogeneous; a dense central granule is normally present distally and less distinct granules and vague fibrous linear structure more proximally (Fig. 7 G). In both centrioles the region below the distal partition has very fine cross-links between triplets on the lumenal side, possibly linking the A-tubules (Figs 7 F,G).

The posterior centriole attaches to the anterior centriole surface at its approximate middle part, the angle between them generally being 90° (Figs 7 F—H, 8 F). Centrioles lie nearly in one plane (dorsal—ventral, turned to the left with the anterior one offset a third of a diameter to the left). The posterior centriole points ventrally and backwards; the anterior centriole points to the left and forwards (Figs 4, 5). Each centriole has a short fibrillar foot (ff) to the left-posterior side of the cell (Figs 7 F,G, 8 A). The feet fuse together at their distal ends, and initiate the left anterior root (lr), which consists of two microtubules within dense material that often largely obscures them. The two microtubules are best seen at its origin (Fig. 8 A) and at the most distal part (lr; Fig. 7 C), but in its middle part are so-filled with dense material that they can rarely be recognized; the left anterior root is normally like a thick fibre or strip (Fig. 8 C). The anterior centriole's 2—3 fibrillar feet are a bit distal to the cartwheel; the fibrillar foot of the posterior centriole is attached to the left side of its basal transverse plate and is longer and broader at its distal end (Figs 7 F,G, 8 A—C,F). The left anterior root passes from the foot fusion point forward alongside the anterior centriole, turning slightly leftwards. It attaches to the cell surface connecting the centrioles to the plasma membrane and continues some distance alongside the anterior flagellum (Figs 7 C—F). This left root gives rise along its length to many single variously directed microtubules (sml; Figs 8 D,E). Its proximal part

produces a band of 6—9 secondary microtubules (dsm) passing dorsal and backwards deep into the cell (Figs 7 F—I, 8 A,B,F). A short, striated, ventrally directed spur is near the proximal end of the anterior centriole, posterior to the left root origin (fsr; Figs 7 B,H, Fig 8B).

The short dorsal anterior root (da) of two microtubules nucleates from the right of anterior centriole (Figs 7 D—H), opposite the posterior centriole, and passes forward and slightly to the left. It attaches to the plasma membrane, where it seems to end, and may produce secondary single microtubules passing backwards into the cell — some pass from the base of this root in the nuclear direction as a microtubular cone (mc, Fig. 8 A).

One major ventral root (VP2), initially of three microtubules, originates from the left dorsal side of the anterior centriole, connecting to a thin dense fibrillar sheet on the dorsal side of the anterior centriole (Figs 6, 7 B,H, 8). The microtubules in VP2 increase to six. An ER cisterna usually applies to root VP2 (Fig. 8 F).

The second major ventral posterior root (VP1) of five microtubules starts from fibrillar material around the posterior left surface of the posterior centriole, passing backwards alongside it and root VP2 (Figs 8 D,E). At its origin VP1 also connects with a dense plate attached to the posterior centriole by fibrillar bridges (fb; Fig. 8 C). Root VP1 sharply turns from being perpendicular to the axis of the anterior centriole and roughly 45 degrees to the axis of the posterior centriole at its origin to parallel to it, then follows the posterior centriole and flagellum, between the plasma membrane and VP2 (Figs 7 B,G—I, 8 D,E). VP1 microtubules may increase to 7. At the level of the posterior flagellum/centriole junction both ventral roots split into two branches underlying the plasma membrane of the flagellar groove. Root VP2 is leftward of VP1. In some sections we found these VP microtubules at the middle and even in the posterior part of the cell.

A more distinct posterior pair of secondary microtubules passes from the anterior centriole along the posterior centriole in the same direction as, but well to the left of, the ventral posterior roots (sml; Figs 8 D,E). A broad indistinct fibrillar root of amorphous material (fr; Figs 7 B,G,H) passes from the left-posterior side of the anterior centriole and splits into two branches: a broad one directed to the nucleus and a narrow, dense branch alongside VP2. The nuclear projection ends very near the VP1/VP2 association (Fig. 7 H), where the dense branch ends.

Cercomonas strain RS/21 (Fig. 9)

The structure and disposition of organelles, including the flagellar apparatus, are very similar to those of strain C-84 (Figs 9 A,O,P), but mushroom-like bodies were not found. Transition zones of both flagella have concentric rings; each centriole has a thick distal partition with diaphragm (Figs 9 D,N,P). A cartwheel is in the proximal quarter of the anterior centriole only (Figs 9 H,N,O). The proximal partition of the posterior centriole has a less prominent projection than in C-84 (Fig. 9 O). The posterior centriole attaches to the anterior centriole middle; the angle between them is much more than 90° (Figs 9 N—P), not 90° as in C-84. Their interconnecting fibrillar bridges and origin and structure of the microtubular roots, short striated spur, and left fibrillar feet producing the left anterior root are as in C-84 (Figs 9 B—P). The thick amorphous fibrillar root of at least two branches passes from the anterior centriole very close to the nuclear projection and VP2/VP1 association (Figs 9 E,F,L,M,O,P). The microtubular cone is associated with the proximal part of the anterior centriole and its dorsal anterior root (Fig. 9 H). An ER cisterna applies to root VP2 (Fig. 9 K).

Cercomonas strain C-43 (Fig. 10)

General cell structure is as in the previous strains (Fig. 10 A,B), with MRBs as in C-84 (Fig. 10 A). The main difference is the many symbiotic Gram-negative bacteria free in the cytoplasm without surrounding membranes (Fig. 10 A). The posterior flagellum is in a groove or channel supported by microtubules of roots VP2 and VP1 (Fig. 10 K). Flagella and centrioles are as in C-84 and RS/21. The angle between the centrioles is about 120° (Fig. 10 B). In some cells centriole orientation differs from that described above: the anterior centriole points to the left and the posterior centriole backwards, and the plane of both centrioles is parallel to the ventral side of the cell. The anterior connective between the centrioles has thin striations (Fig. 10 B); conceivably it is a contractor to change the angle between the centrioles. All roots are as in C-84 and RS/21 (Figs 10 C—K), including the ER cisterna on VP2. The nuclear projection is much closer to the centrioles and two fibrillar root branches directed to its surface are visible in Figures 10 E and 10 H. The microtubular cone is in different position (Figs 10 D,E,H): associated with fibrillar material around the posterior centriole (Figs 10 D,E), and

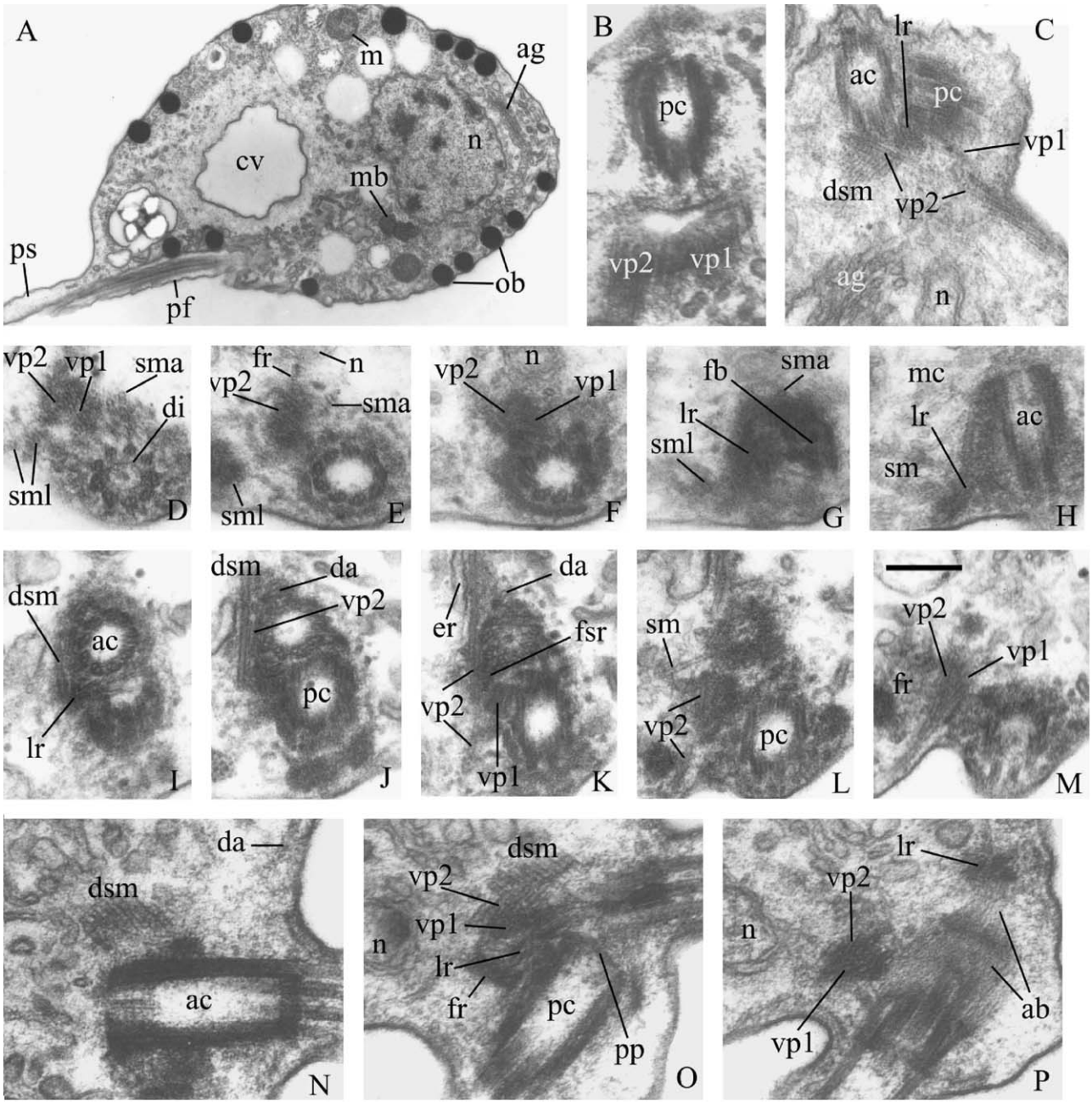

Figure 9. General view and kinetid structure of *Cercomonas* strain RS/21. **A:** General view of the cell in saggittal section. **B:** Oblique section of posterior centriole and divergence of ventral posterior roots (vp1 and vp2). **C:** Section of both centrioles with main roots. **D—H:** Selected consecutive sections of kinetid. **D—G:** Distal to proximal cross sections of posterior centriole (viewed from tip to base). **H:** Oblique section of anterior centriole. **I—M:** Selected consecutive sections of kinetid: **I—L:** Distal to the proximal cross sections of anterior centriole (viewed from base to tip). **M:** Oblique section of the distal part of posterior centriole. **N—P:** Selected consecutive section of kinetid: **N:** Longitudinal section of anterior centriole. **O—P:** Oblique sections of posterior centriole, showing fibrillar connections of both centrioles and disposition of main roots. Scale bar: A — 1 μm; B—M — 200 nm; N—P — 150 nm.

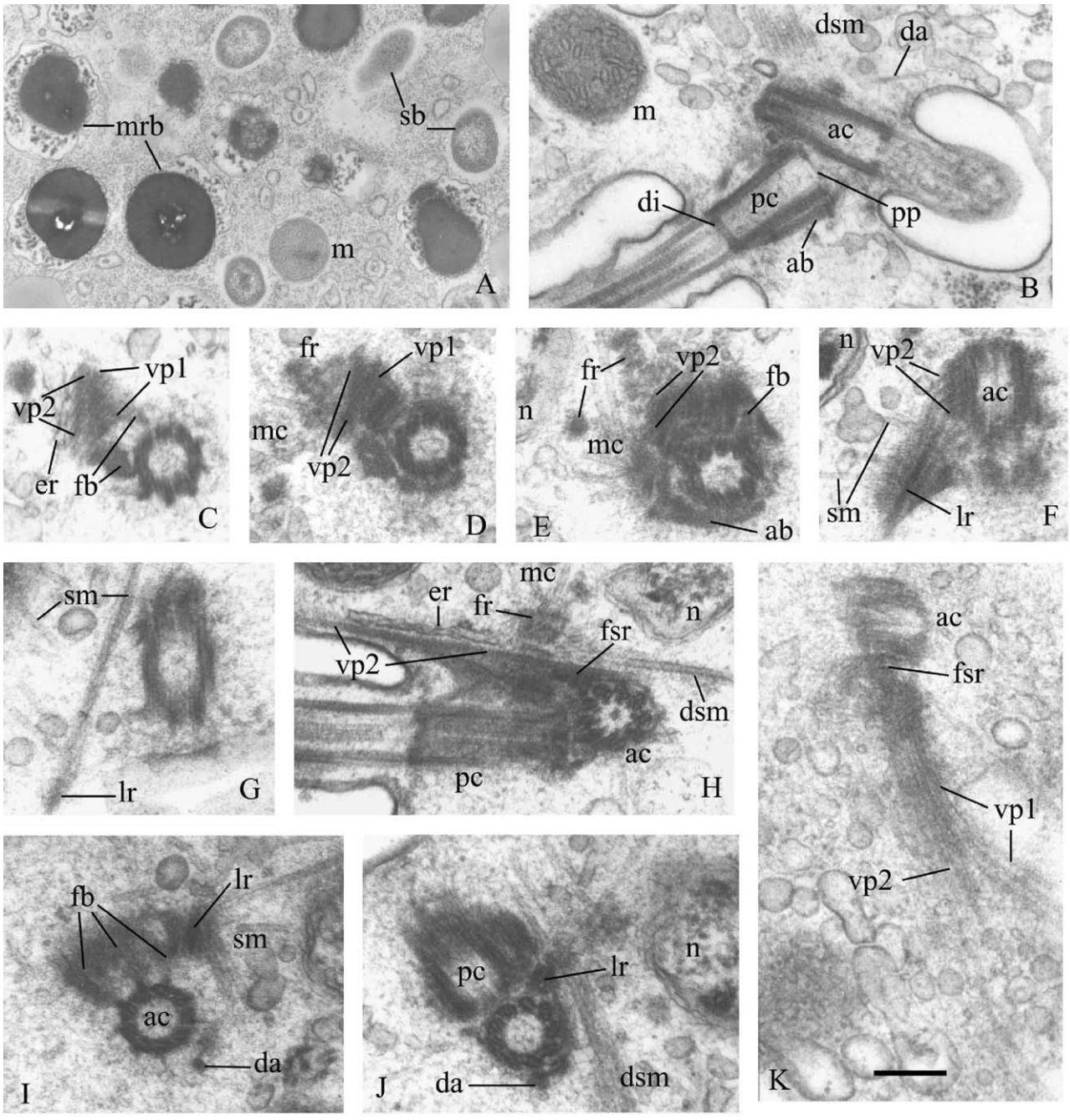

Figure 10. Cytoplasmic organelles and kinetid structure of *Cercomonas* strain C-43. **A:** Portion of cytoplasm. **B:** General view of kinetid; note thin striation of the anterior fibrillar bridge (ab). **C—G:** Selected consecutive sections of kinetid: **C—E:** Cross sections of posterior centriole from distal to the proximal part (view from tip to base). **F—G:** Oblique sections of anterior centriole. **H:** Cross-section of proximal end of anterior centriole. **I—J:** Distal to the proximal consecutive cross sections of the anterior centriole (viewed from base to tip), showing fibrillar bridges (fb) between centrioles and the origin of the left anterior root (lr). **K:** Divergence of the ventral posterior roots (vp1 and vp2). Scale bar: A — 0.5 μm; B—K — 200 nm.

with one branch of the fibrillar root (Fig. 10 H). Single microtubules of this cone pass in different ways, predominantly into the cytoplasm, and to the nucleus (Figs 10 H,J). The thick left anterior root passes from the point of feet fusion forward along the anterior centriole turning slightly

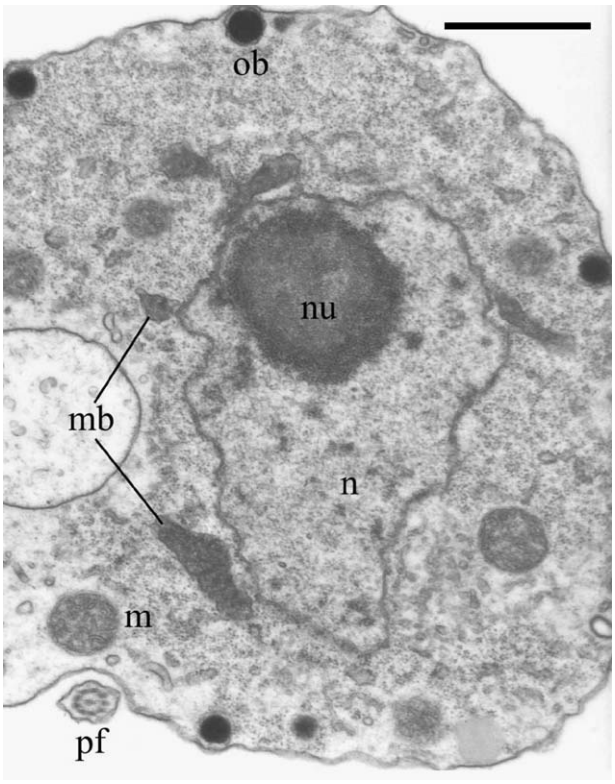

Figure 11. Transverse section of the cell of *Cercomonas* strain C-59. Scale bar: 1 μm.

leftwards (lr; Figs 10 F,G,I,J). It attaches to the cell surface, connecting centrioles to the plasma membrane (Fig. 10 G), and nucleates many variously oriented single microtubules (Figs 10 B,F,J) and a band of six secondary microtubules. A dorsal anterior root of 1—2 microtubules passes from the dorsal part of the sheet forward (da; Figs 10 B,I,J). Roots VP2 of three microtubules and VP1 of 4-5 microtubules are as in other clade A strains. They split into a left and right part, which pass alongside the posterior flagellum (Figs 10 C—E, H, K,).

Cercomonas strain C-59 (Figs 11, 12)

Its general ultrastructure is most similar to C-84 (Figs 11,12 C). The posterior flagellum lies in a groove. Mushroom-like bodies are rare, but very big, sometimes half the nuclear dimension. Centrioles are joined at an obtuse angle. Transition zone and centrioles of both flagella are as in C-84 (Figs 12 A,B,E,F), as is the flagellar root system (Fig. 12) except that the foot of the posterior centriole is not as developed as in C-84—more like that of C-43 and RS/21 (Figs 12 B—D). The fibrillar sheet around the posterior centriole is clear in Figures 12 C and I, which show its structure and connection with microtubular roots. The left anterior and ventral roots VP2 and VP1 have the same position and microtubule number as in previously described strains (Figs 12 A,B,D,J,K). Both ventral posterior roots are accompanied by two strands of two microtubules originating from the left anterior root and base of the anterior centriole respectively (Figs 12 A,E—J). After following the posterior centriole and then its flagellum, VP2 and VP1 diverge to the left and right, and together with secondary microtubules from the left anterior root and anterior centriole form two separate bands underlying the flagellar groove membrane (Fig. 12 D). The number of microtubules may increase to six in VP2 and seven in VP1. Thus the complex posterior band may have 2+7+6+2 microtubules (Fig. 12 E). The unbranched, inconspicuous, amorphous nonstriated fibrillar root passes from the centrioles towards the nucleus (Fig. 12 C). Roots VP2/VP1 associate with the nucleus as in C-84 (Fig. 12 E). An ER cisterna is on VP2 (Fig. 12 A). The microtubular cone is not well developed; its microtubules associate with the anterior centriole (Fig. 12 D).

Eocercomonas ramosa: strain C-80 (Figs 13, 14)

This strain differs from all the others in general morphology and flagellar apparatus structure. The nucleus contains prominent peripheral and much interstitial heterochromatin (Fig. 13 A). Neither a nucleolus nor a nuclear projection towards the centrioles is evident. A large Golgi dictyosome is applied to the anterior ventral part of the nucleus. Mitochondria predominantly have tubular cristae, some branched (Figs 13 A,J). Microbodies are not prominent, but near the nucleus. No extrusomes were found. Mushroom-like bodies are scattered through the cytoplasm. Its most peculiar feature is a prominent rough ER cisterna around the nucleus and part of the surrounding cytoplasm (Fig. 13 A). The posterior flagellum lies in a groove supported by microtubules.

The transition zone of both flagella is short. A very thin transverse plate is at the distal end of the centriole, level with the transitional fibres connecting it to the plasma membrane (Figs 13 K,M). In marked contrast to all clade A1 strains there is no thick distal partition with obvious peripheral diaphragm. A concentric fibre or ring is above the

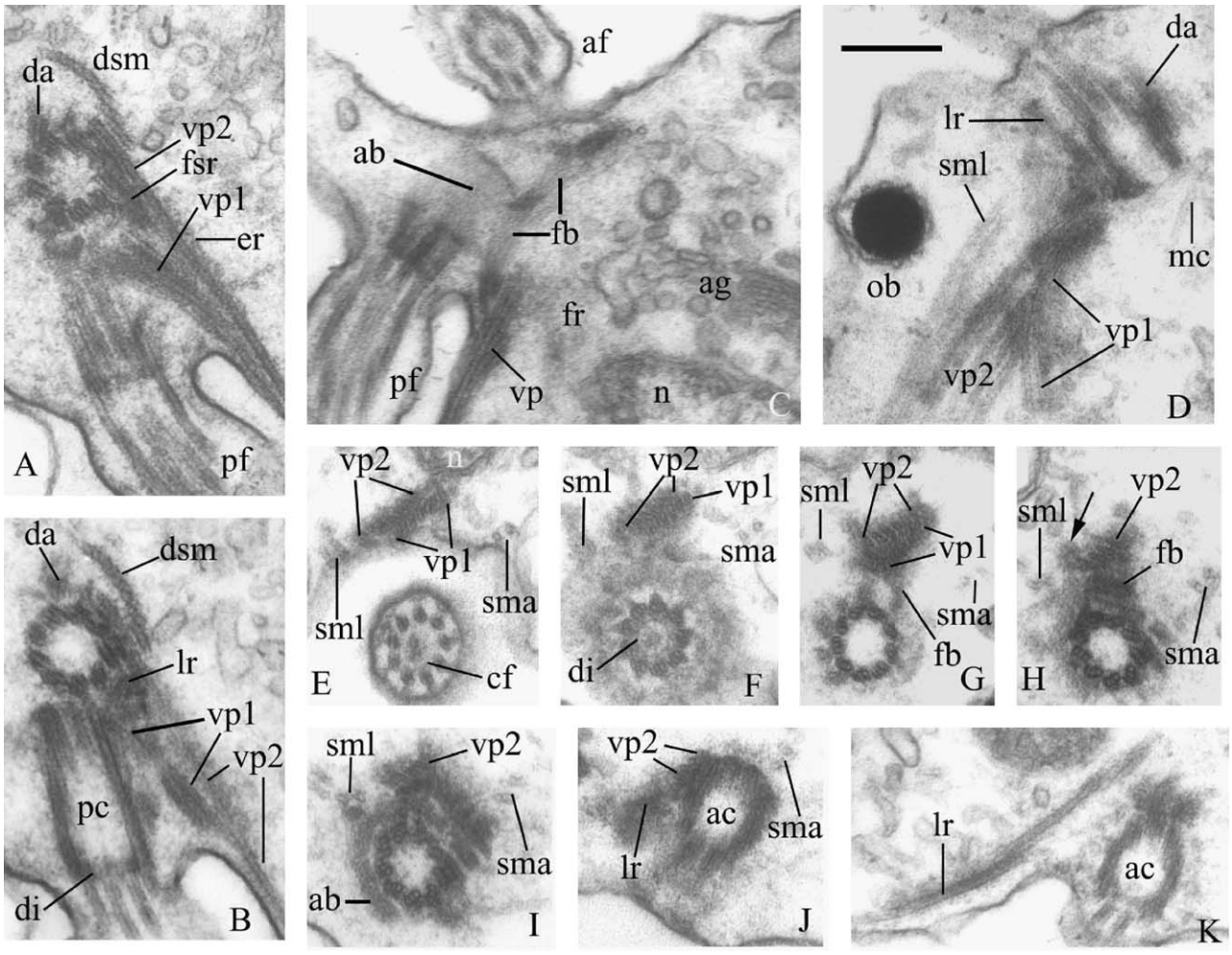

Figure 12. Kinetid structure of *Cercomonas* strain C-59. **A—B:** Proximal to the distal consecutive cross sections of anterior centriole (viewed from tip to base) showing the main roots. **C:** Fibrillar connections of posterior centriole. **D:** Divergence of ventral posterior roots (vp1 and vp2). **E—K:** Selected consecutive sections of kinetid: **E—I:** Cross sections of axoneme and posterior centriole from distal to the proximal part (view from tip to base), **J-K:** Oblique sections of anterior centriole. Scale bar: A—K — 200 nm.

transverse plate (Figs 13 B,C). A cartwheel was not seen in any centrioles (Figs 13 G,H,K), but a basal partition is present in both. The posterior centriole has a sheet of fibrillar material around its ventral left surface, continuing into an anterior fibrillar bridge as in other strains (Figs 13 F—H). The posterior centriole attaches to the anterior centriole's posterior middle surface, the angle between them being over 90°. Fig. 14 is a reconstruction of the roots, clearly very different from the other strains (Fig. 6). The anterior centriole has three microtubular roots. The dorsal anterior root of at least one microtubule passes forwards and leftwards beneath the plasma membrane. A VP2 root of 2—3 microtubules starts from the left side of the anterior centriole and passes backward alongside the posterior centriole (Figs 13 I,L,M). A dorsal posterior root of four microtubules originates from the middle right dorsal side of the anterior centriole, passing back to support the dorsal side of the cell (Figs 13 I,J).

A small fibrillar projection (like a fibrillar foot) from the right dorsal side of the anterior centriole's proximal end (ff; Figs 13 H,J) produces a cone of microtubules from its distal end (mc; Fig. 13 I). It is associated with the dorsal posterior root and another fibrillar foot coming from the anterior centriole to the right. A similar projection comes from the posterior centriole and fuses with that foot, forming a small granule at the end. A thinly

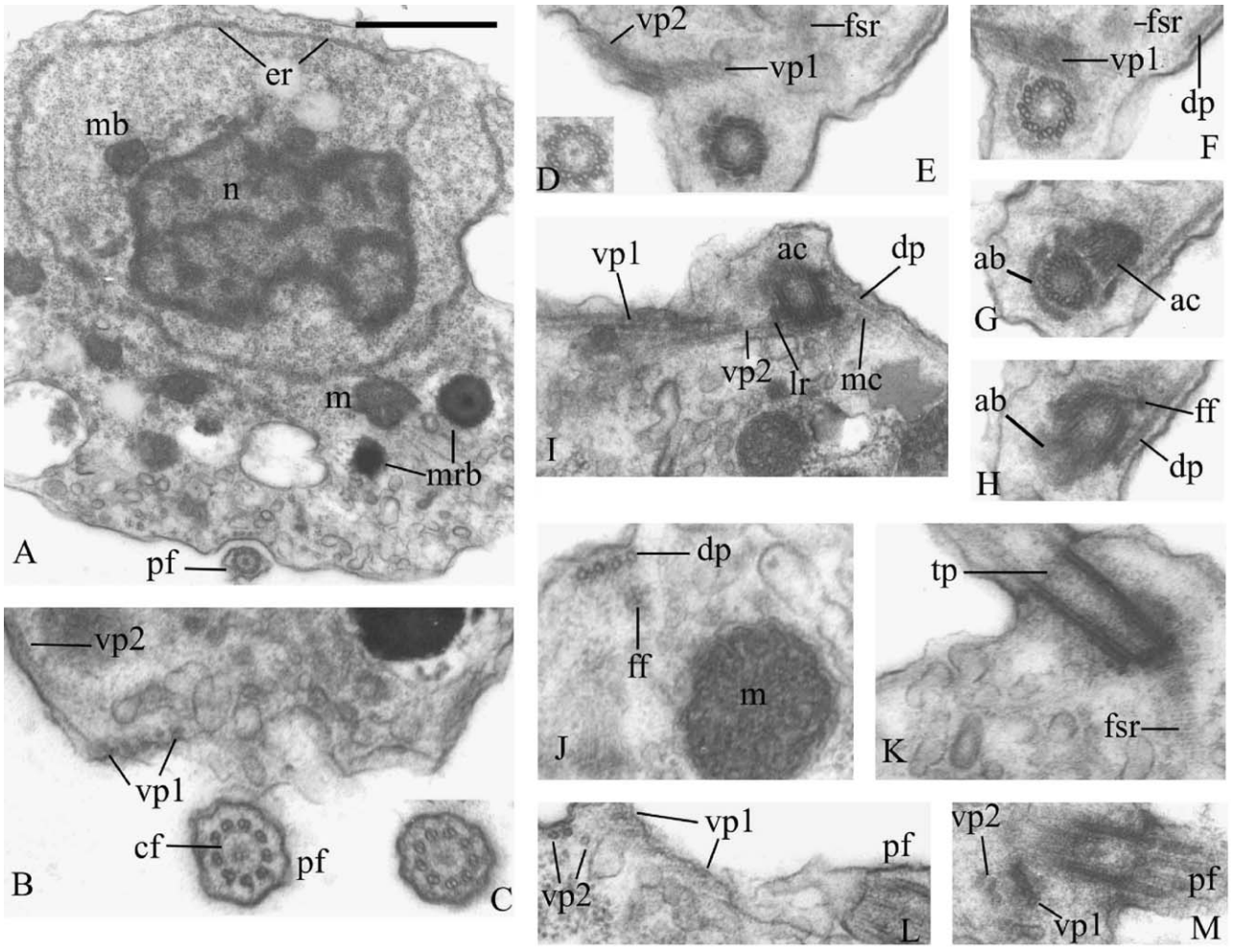

Figure 13. General view and kinetid structure of *Eocercomonas ramosa* strain C-80. **A:** Transverse section of the cell. **B—H:** Series of consecutive sections of kinetid. **B—G:** Distal to proximal cross sections of axoneme and posterior centriole (viewed from tip to base). **G—H:** Oblique sections of anterior centriole. **I:** Roots associated with anterior centriole. **J:** Section next to the proximal end of the anterior centriole. **K:** Anterior centriole longitudinal section. **L—M:** Selected sections from one series, showing divergence of ventral posterior roots. Scale bar: A — 1 μm; B—C, K—M — 350 nm; D—I — 400 nm; J — 300 nm.

striated fibrillar root passes from this granule deep into the cell towards the nucleus (fsr; Figs 13 E,F,K). The posterior centriole has only a VP1 root of four microtubules passing from its middle dorsal right surface backwards along the posterior centriole and VP2. At the level of the distal end of the posterior centriole VP1 has five microtubules and VP2 has three. Posterior to the posterior centriole a VP2 root underlies VP1 as in other strains (Fig. 13 M). Distally both roots mutually diverge, taking different directions beneath the plasma membrane (Figs 13 B,L); they lack secondary microtubules. The short left anterior root is inconspicuous with only one microtubule and no secondary ones (lr; Fig. 13 I). It originates from the fusion of fibrillar feet as in other strains (Fig. 13 G). There is no short striated fibrillar root (spur) on the anterior centriole.

Taxonomy

The marked differences in fundamental morphology shown above within the classical genus *Cercomonas*, as well as the deep sequence divergence between clade A and B shown previously (Bass et al. 2004, 2005; Cavalier-Smith and Chao 1996/7, 2003; Ekelund et al. 2004) and between A1 and A2 and B1 and B 2 shown above,

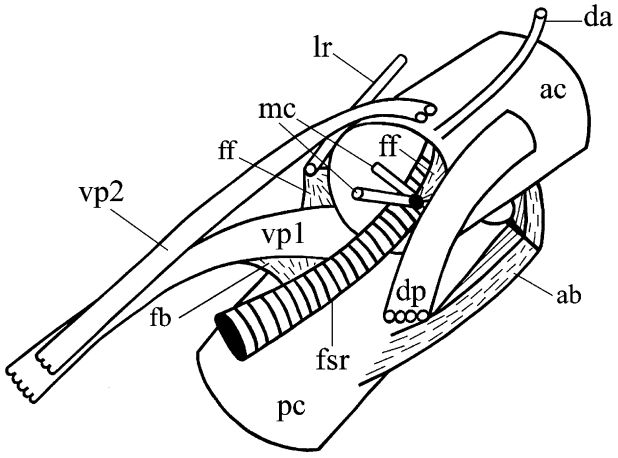

Figure 14. Reconstruction of kinetid structure of *Eocercomonas ramosa* strain C-80 (clade A2). Viewed from above (dorsal side) but from the right (i.e. at an angle intermediate between Figs 5 A and B; for abbreviations see Fig. 5 legend).

make it highly desirable to subdivide this unduly broad genus into several separate genera. But this cannot be done without determining to which clade the type species *C. longicauda* (thus designated by Fromentel (1874), according to Ekelund et al. 2004) belongs, since only that clade can retain the name *Cercomonas*. Thus no progress can be made in revising the high level classification of Cercomonadidae without identifying a strain that is *Cercomonas longicauda* Dujardin. This is less easy than Ekelund et al. (2004) assumed, as almost every author since Dujardin (1841) has had a different idea of what *C. longicauda* looks like. For example *C. longicauda* of Lemmermann (1914; fig. 59, p. 48, as *Cercobodo longicauda* for which he gave the authority (Klebs) Senn contrasting with (Stein) Senn in the text!) is so dramatically different from Dujardin's description and figure that it cannot be the same species. Fig. 4 L reproduces Dujardin's figure (scanned digitally and unchanged except for contrast enhancement). The anterior flagellum is about 3.8 × the body length and the clearly visible posterior flagellum projects a full body length behind the cell; hence the name *longicauda*. Furthermore the flagellum adheres to the cell body right up to its extended posterior tip. None of these three characters, the only distinguishing features of Dujardin's *longicauda* apart from cell size, is true of Lemmermann's figure nor of either the SCCAP strain (see fig. 5 of Ekelund et al. 2004, where the elongated posterior of the cell and the flagellum are clearly distinct and the posterior flagellum does not project beyond it) or the ATCC strain (see Fig. 4 J—K). All three strains have an anterior flagellum about equal to the body, not 3.8 × its length as in Dujardin's figure (or 3—4 ×, implied by his description). Thus all three were certainly misidentified as *longicauda*. None of them has the projecting posterior flagellum that obviously caused Dujardin to confer that name in particular. Translated into English, Dujardin's complete diagnosis of *C. longicauda* is:

> Flexible spindle-shaped body, terminated at the rear by a very thin flexuous filament in the form of a tail. Body length 8—9 μm. Tail [i.e. the projecting part of the posterior flagellum] 15 μm. Flagelliform filament [i.e. anterior flagellum] very thin, 30—40 μm.

Ekelund et al. (2004) did not explain why they identified their strain as *longicauda*, and made no comparison with Dujardin's original description, nor cited it. The only previous description they referred to was by Sandon (1927, p. 72), who gave a body length of 5—10 μm, and 3—4 × body length for the anterior flagellum (a marked discrepancy with the SCCAP strain; Ekelund et al. 2004) and 'slightly longer than body length' for the posterior flagellum. Although the SCCAP, ATCC, and Lemmermann (1914) strains are mutually similar in flagella/cell proportions and in the protoplasmic tail often obscuring the no longer posterior flagellum, they all differ in size from each other and Dujardin's. Lemmermann's strain is the largest (18—36 μm), SCCAP the smallest 4—10 μm, and ATCC intermediate (10—12 μm).

Ekelund et al. (2004) designated their SCCAP C1 as 'neotype' for *C. longicauda*, even though it differed in every respect except size from *C. longicauda* Dujardin, 1841. They also did not expressly explain why neotypification was necessary or explicitly meet all seven of the conditions that the International Code of Zoological Nomenclature (ICZN) requires for designation of a neotype. Thus SCCAP C1 is invalid as a neotype for *C. longicauda*. As only a valid neotypification has authority, this still remains to be done. Because of the exceptional importance of stabilizing the application of the name *Cercomonas* before the taxonomy of Cercomonadidae can be revised, it is necessary to designate a valid neotype for *C. longicauda* here.

In recent decades four different clonal strains have been contradictorily identified as *C. longicauda*. Both of those that belong in clade B1 (SCCAP C1 and ATCC 50344) were definitely

misidentified. Strain C-1 (now dead) of Mylnikov (1987), with ultrastructural features suggestive of clade A1 not clade B — see discussion, was probably also misidentified, as *C. longicauda* sensu Mylnikov (2000) was 18—36 μm — far larger than Dujardin's; its large size and ultrastructure together suggest that it belongs to clade A1b (see above), but it was distinct from all three A1b strains in Figure 3. CCAP 1910/2 *longicauda*, less obviously misidentified, is in clade A1a. The very same excessive dimensions (18—36 μm) were given by Klebs (1892), whose drawing differed greatly from Dujardin's, and by Zhukov (1993) with drawings of *longicauda* (after Skuja, but essentially the same as Klebs) also nothing like Dujardin's, but not unlike *C. ekelundi*; Kent's (1880—2) drawings differ in showing a distinct posterior flagellum, but appear to have been copied from those of Stein (1878), which also are probably not of the same organism as Dujardin's. The use of conflicting secondary sources for identification has led to many different organisms being wrongly identified as *longicauda* and *crassicauda* (the only two species in Stein's treatise that can be accepted as *Cercomonas*). We heartily concur with the comments that 'more than one species may be included' among the numerous records of this 'species' (Al-Qassab et al. 2002), and that most (if not all) are 'highly questionable' (Foissner 1991). The fact that four such different cultures of cercomonads, belonging in three radically different parts of the tree, have been identified as *longicauda* (three certainly incorrectly), and the numerous discordant drawings and descriptions in the literature, emphasize the urgent necessity to clarify and standardize the taxonomic status of *C. longicauda*. This is best done by designating a neotype much closer to Dujardin's original description than is SCCAP C1, even though certainty that it is the same species is unattainable.

Neotypification of *Cercomonas longicauda* Dujardin 1841

Conditions of article 75.3 of ICZN for valid typification are met thus:

1. We designate the CCAP 1910/2 culture as the hapantotype and neotype for *C. longicauda* Dujardin 1841 for the express purpose of clarifying the taxonomic status of that species.
2. *Cercomonas longicauda* can be distinguished from all other species by its 18S rRNA sequence. Any strains differing by 3 nucleotides or more are to be regarded as different species (except for any that might in future be shown to be sexual and able to interbreed freely with it).
   Description of the neotype strain: Cell ~8—10 μm long when gliding, often amoeboid. Its posterior flagellum adheres strongly to its body and extends about a body length (i.e. its total length is 15—20 μm) beyond its posterior tip and is thus always clearly visible during gliding motion, when its body is spindle-shaped (Figs 4 U,V). Its anterior flagellum is about twice its body length (usually 15—17 μm). Cysts are spherical and smooth walled. Contractile vacuole. Pseudopodia broad, flat and lobed (Figs 4 W, X). Nucleus anterior. Cells sometimes clump together (Fig. 4 Y). Plasmodial stage compact and rounded, not a string of almost separate cells (Fig. 4 Z).
3. The neotype is strain CCAP 1910/2 isolated by Zölffel in 1991, and could also be recognized by its 18S rRNA sequence together with a light microscope appearance as described above and shown in Figures 4 U—Z, even if it were mislabelled in future. Thus recognition of the neotype designated is assured.
4. There is no reason to think that Dujardin ever made any type specimens of any of the protozoa that he described. Thus no holotype ever existed. Designation of a neotype by Ekelund et al. (2004) is invalid, as the designated strain was misidentified and definitely not *longicauda* as described by Dujardin (1841) (see above).
5. Half the 22 strains studied here (all in Fig. 3 except *plasmodialis*, C-43 and C-85, plus *longicauda* in Fig. 4 U—Z) are substantially more like Dujardin's description than is SCCAP C1.

Several are totally indistinguishable from Dujardin's in body form and size (e.g. CeS-2, C-72, NZ1, *longicauda* CCAP1910/2). However, all differ in having somewhat shorter anterior flagella and sometimes also somewhat shorter posterior flagella. This makes it possible that none of them is really precisely the same as Dujardin's. However, this leaves out of account the probability of variation in flagellar lengths within a clone and the fact that Dujardin's description was not based on clonal cultures anyway, and we cannot know how representative the individual cell that was figured was. We point out, for example, that the individual cell of C-80 in Figure 4 A (photographed in the Borok lab) has an anterior flagellum over

three times its body length, yet most gliding cells of this strain growing in the Oxford laboratory have anterior flagella less than twice the body length, as do several several cells in the plasmodial phases depicted in Figure 4 D. Thus, even within a clonal *Cercomonas* culture, there can be discrepancies in anterior flagellum length as great as the differences seen between several clade A1 cultures and Dujardin's. Thus, for most of these cultures it could not be argued with confidence that they are not the same species as Dujardin's. Thus several of them could reasonably be chosen as a neotype. Conversely, however, the fact that so many clade A1 cultures are almost indistinguishable except for anterior flagellum length from Dujardin's *longicauda*, yet have very different rRNA sequences and must virtually all be different species from each other and from his, makes selection of a specific one essentially arbitrary. We shall never know what was the rRNA sequence of Dujardin's strain, nor whether the strain he observed had plasmodial phases and cysts or not. Yet the need to chose a neotype and stabilise nomenclature is so great that one must be chosen, even though their morphological similarity necessarily gives inadequate morphological basis for doing so. We have over a hundred other *Cercomonas* cultures in the Oxford laboratory, nearly half of which would be almost as suitable, but none of which ordinarily have anterior flagella 3—4 times body length.

We therefore designate CCAP 1910/2 as neotype not only because (apart from its usually somewhat shorter anterior flagellum) it is indistinguishable from the original description, but also because it is quite closely related to RS/21, which we have now well characterised ultrastructurally, and RS/22, both of which have been used for characterising protein genes as well as rRNA (Archibald et al. 2003; Bass et al. 2005; Cavalier-Smith and Chao 1996/7; Keeling 2001). However, CCAP 1910/2 is preferable to either RS/21 or 22 as it is already available from CCAP and has survived there for 14 years of subculturing after its was isolated and identified as *longicauda* by an independent *Cercomonas* expert, Zölffel. The latter is important as ICZN also recommends (article 75B) that expert opinion be sought to verify 'that the proposed designation does not arouse serious objection from other specialists in the group in question'. Accordingly we also consulted K. Vickerman (Glasgow), who agrees that this strain would be an acceptable neotype and that SCCAP C-1 from Danish agricultural soil, and the ATCC strain (a marine strain, unlike Dujardin's, with distinctly non-adherent posterior flagellum) especially, were both misidentified.

The species *C. longicauda* was originally described from three infusions of licorice, gum or potato in Rennes, France (Dujardin 1841; p. 290, Plate 4:15) and thus likely to have come from soil or freshwater; the neotype was isolated by Zölffel in 1991 in England from freshwater (http://www.ccap.ac.uk). Zooflagellate morphospecies are widely thought to be cosmopolitan (Finlay 2002; Finlay and Clarke 1999). Although this need not be the case for species defined by more discriminating molecular methods (Cavalier-Smith and Chao 2006; von der Heyden and Cavalier-Smith 2005), for at least a few *Cercomonas* strains we have been able to recover precisely the same *Cercomonas* 18S rRNA sequence from samples on different continents as far apart as England, Panama and New Zealand, so there is currently no sound reason to think that designating a neotype from a different locality matters in any way or that ignorance of the precise location of either the neotype or original is relevant to their identity.

The neotype culture is available from CCAP (http://www.ccap.ac.uk).

Cercomonas Dujardin 1841 emend. Karpov, Bass, Mylnikov, and Cavalier-Smith (non-*Cercomonas* emend. Ekelund et al. 2004), revised diagnosis

Gliding, typically spindle-shaped cercomonads with the posterior flagellum trailing, usually extending behind the cell body. Broad, flat lobed pseudopods or filopodia often formed, usually unbranched. A prominent nuclear extension directed to the nearby centrioles. Tubular mitochondrial cristae usually slightly flattened. The anterior centriole usually has a proximal cartwheel but the posterior one does not. Both centrioles have a thick distal partition with a more prominent diaphragm-like outer part. The anterior centriole has a fibrillar striated spur. Posterior centriole only has a proximal transverse plate. Extrusomes are nearly isodiametric osmiophilic bodies. Some species have a complex life cycle including multinuclear plasmodia and spherical cysts (smooth-walled or rugose). With three diagnostic signature sequences in 18S rRNA: CATT, GAGGGACTATCGGT$_C$GATTTA (N1 of Ekelund et al. 2004), and GGACT (see Table 1). N2 of Ekelund et al. (2004) is not diagnostic for clade A1 on our rRNA trees. Type species *C. longicauda*

Dujardin 1841, with neotype culture CCAP 1910/2 and type sequence: DQ442884.

Cercomonas jutlandica (Ekelund et al.) comb. nov. Cavalier-Smith and Bass

Basionym *Neocercomonas jutlandica* Ekelund et al. (2004 p. 129). As the type species of *Cercomonas* (*C. longicauda* Dujardin) falls within the original definition of *Neocercomonas*, *Neocercomonas* is now a junior synonym of *Cercomonas*. But it remains available as a potential generic or subgeneric name for a differently defined restricted subset of clade A1 excluding *longicauda* but including *jutlandica* (e.g. clade A1b), should it be needed.

Eocercomonas **gen. nov. Karpov, Bass, Mylnikov, and Cavalier-Smith; Diagnosis**

Gliding, typically spindle-shaped cercomonads with the posterior flagellum trailing as in *Cercomonas* and *Paracercomonas. Eocercomonas* differs from both these genera in having a dorsal posterior microtubule band and nuclear fibrillar striated root. It differs from *Cercomonas* in lacking a nuclear extension to the centrioles, and in lacking cartwheels in both centrioles and having a proximal transverse plate in the anterior as well as the posterior centriole, thin distal centriolar partition (without peripheral diaphragm), and a long fibrillar striated root passing from the posterior centriole towards the nucleus, and mitochondrial cristae are rounded tubules. With three diagnostic sequence signatures in 18S rRNA: TAATT, TCGAGC$_T$TTACAACCTTGACT, and CTT$_C$CTGTTCTATTTGTTGGTTTCTAGGAT$_C$GG (see Table 1). Type species *E. ramosa* sp. nov. Corresponds with clade A2 on our rRNA trees. Etym. *Eo*- Gk. dawn, *Cerco* — Gk tail; *monas* Gk unit, because it is a tailed monad that is sister to *Cercomonas sensu stricto* and diverged from it before any *Cercomonas* species separated from each other. A feminine noun, like *Cercomonas* Dujardin.

Eocercomonas ramosa sp. nov. Karpov, Bass, Mylnikov, and Cavalier-Smith; Diagnosis

Gliding cells spindle-shaped, 5—15 μm long. Proximal part of anterior flagellum surrounded by a cytoplasmic sheath. Anterior flagellum usually over twice body length when actively gliding (>20 μm). Posterior flagellum almost invisible, protruding only slightly behind cell. Contractile vacuole in the anterior part of the cell. Extrusomes absent. Trophic cells produce highly branched very slender pseudopodia, and may group together in consortia. Dorsal anterior root laterally attached to anterior centriole. Cysts unknown. Etym. *ramosa* L. = branching, because of its branching filopodia. Type strain C-80 isolated from a freshwater lake in Antarctica by A.P. Mylnikov. Type illustrations Figures 4 A—D. Type 18S rRNA sequence AY884327.

Cercomonas (= *Cercobodo*) *cometa* (Hollande) is the most similar named species but differs in its relatively shorter anterior flagellum and, notably, its posterior flagellum being equal to or longer than the anterior one. We prefer to designate the whole 18S rRNA sequence as the type because there is a danger that if one picks just one or two highly variable segments that could inadvertently include several different related ribotypes.

Paracercomonas **gen. nov. Cavalier-Smith and Bass; Diagnosis**

Gliding, with flexible very metabolic body usually able to produce pseudopodia of different shapes, including branched filopodia, from any part of the cell. During movement the cell body attaches to the substrate. Anterior flagellum makes slow rowing motion, posterior flagellum trails behind more passively. Mitochondrial cristae rounded tubules. Some species have complex life cycle including multinuclear plasmodia and cysts. Distinguished from *Cercomonas* and *Eocercomonas* by usually having cartwheels in both centrioles and by a diagnostic, highly conserved, and derived complementary base-pair substitution U—A base pair at base pair 7 in helix 25, instead of a G—C pair as in all other cercomonads (see Table 1 and preceding analysis). Corresponds with clade B1 on our rRNA trees. Etym. *Para*- Gk. beside, contrary to; *cerco* — Gk tail; *monas* Gk unit, to emphasize that it is probably sister to *Cercomonas* plus *Eocercomonas*, but more dramatically different in sequence and to some extent morphology than they are from each other. A feminine noun, like *Cercomonas* Dujardin.

Paracercomonas marina sp. nov. Cavalier-Smith and Bass; Diagnosis

Cercomonad with irregular, sometimes lobed or truncated, posterior, slightly longer than and often

entirely obscuring its slightly shorter posterior flagellum. Body length ~10 μm; anterior flagellum ~10 μm. Unambiguously distinguishable from morphologically similar species, e.g. the slightly larger *P. ekelundi* by its 18S rRNA sequence. Plasmodial stage, contractile vacuole or cysts unrecorded. Marine. Type culture ATCC 50344; type 18S rRNA sequence AF411270; type figure Figure 4 J—K.

Paracercomonas ekelundi sp. nov. Cavalier-Smith and Bass; Diagnosis

Cercomonad with narrowly drawn out, sometimes forked, posterior, slightly longer than and often obscuring its similar length (or somewhat longer) posterior flagellum. Body slender, fusiform when gliding, length 10—16 μm; anterior flagellum ~10 μm. Unambiguously distinguishable from morphologically similar species, e.g. the slightly smaller *P. marina* by its 18S rRNA sequence. Contractile vacuole lateral; close to, usually behind nucleus. Soil habitat. Spherical 3—4 μm cysts. Plasmodial phase unknown. Type culture SCCAP C1; type 18S rRNA sequence AY496047; type figure figure 5 of Ekelund et al. (2004). Both *P. marina* and *P. ekelundi* are unambiguously distinguishable from *C. longicauda* by not having a longer posterior flagellum that extends a body length behind the posterior tip of the cell and by its typical non-adherence to that tip.

Paracercomonas metabolica (Mylnikov) Cavalier-Smith and Bass comb. nov.

Basionymn: *Cercobodo metabolicus* Mylnikov (1992). As we have shown that Mylnikov's *C. metabolicus* strain Cs-9 falls robustly in cercomonad clade B1b and has the B1 sequence signature and the *Paracercomonas* sequence signature defined above (Table 1, Fig. 1), it must be transferred from *Cercomonas*, where Karpov and Mylnikov (2004) placed it (as *Cercomonas* (= *Cercobodo*) *metabolicus*; note that although some later authors (Kent 1880—1882; Lee and Patterson 2000) have treated *Cercomonas* as masculine, its originator Dujardin (1841) clearly treated *Cercomonas* as feminine, so it should have been *Cercomonas metabolica*; all other names of '*Cercomonas*' species originally described as *Cercobodo* (treated by Lemmermann, 1914 as masculine and Hollande, 1932 as feminine! Type *Cercobodo laciniaegerens* Krassilstschik, 1886, gender unclear) but since transferred to '*Cercomonas*' with species names ending in —*us* (Mylnikov and Karpov 2004) should similarly be corrected to —*a*.

Discussion

Ekelund et al. (2004) wrote that their 'analysis strongly suggest that *Cercomonas* is not a monophyletic group' and gave that as the prime reason for dividing *Cercomonas* into two genera. However, the failure of clades A and B to group together on their trees and on some, but not all, previous trees (Cavalier-Smith and Chao 2003) is probably a long-branch tree-reconstruction artifact caused by the more rapid evolution of clade B. Their analysis did not strongly argue against monophyly. Only their parsimony trees gave moderate support to the polyphyly or paraphyly of *Cercomonas*. There was no bootstrap support for this in their distance or maximum-likelihood analyses, which were technically superior by allowing for intersite variation. Holophyly of the classical genus *Cercomonas* was found on a maximum-likelihood tree (Cavalier-Smith and Chao 2003), on a gamma-corrected distance tree with massive taxonomic sampling (Bass and Cavalier-Smith 2004), and on a taxonomically rather well-sampled Bayesian tree (Bass et al. 2005). Although statistical support in each case was weak, this consistency among very well sampled trees using the theoretically best methods means that there is no good reason not to continue to regard Cercomonadidae as holophyletic.

Division of *Cercomonas* into separate genera must therefore depend on their morphological and genetic disparity, not on suggestions of polyphyly probably based on computational artifacts. Our phylogenetic, sequence signature, and ultrastructural analyses all support treating clades A1, for which we reserve the name *Cercomonas*, and clade A2 (*Eocercomonas*), and B1 (*Paracercomonas*) as separate genera. Even though we unfortunately cannot accept the name *Neocercomonas* (Ekelund et al. 2004) for clade A1, as that clade includes the type species of *Cercomonas*, *Neocercomonas* could become a useful name for clade A1b, e.g. should it prove desirable in future to establish separate subgenera (or even genera) for A1a and A1b. Our sequence and ultrastructural studies have thus resulted in *Cercomonas* being divided into three very distinct genera. Although this reflects a large advance in evolutionary understanding of the family Cercomonadidae,

the division of *Cercomonas* into two genera by Ekelund et al. (2004) and three by ourselves has the unfortunate practical consequence that cercomonads can no longer be assigned to a genus by light microscopy alone, and we do not know to which of the three genera most named species belong — though we suspect that most will belong to *Cercomonas* and not require renaming. We suggest that the vernacular name cercomonad, corresponding to the family name Cercomonadidae, be used specifically to embrace all three genera and not in a broader sense for a still larger group of Cercozoa. We also suggest that names of cercomonad species not yet assigned to genera are placed in inverted commas. Inability to assign named species to genera is not a serious scientific problem, because one major conclusion from our work must be that no ecological or other observations on *Cercomonas* can be very useful unless the strain being studied is placed on the rRNA tree. Sequences rather than light microscopic characters are the only way of adequately representing the huge biological diversity of this family. New genera will also be needed after further research for the anaerobic cercomonad and for the clade that includes the Tempisque strain.

Our culturing, light microscopy and sequencing have revealed a large number of new '*Cercomonas'* strains. Except for C-56 and C-72, which have identical 18S rRNA sequences, the sequences represented on Figure 1 are so different that there must be at least 50 separate species. Our light microscopy indicates that although some are morphologically very distinct, other superficially very similar strains, e.g. C-71 and C-80 both resembling '*C. cometa'*, can be as genetically distant as any '*Cercomonas'*. This is not surprising since cercomonads can vary visibly in the light microscope in fewer different ways than the 678 variable positions in their 18S rRNA. Apart from size and shape of the flagellates and cysts and the length of each flagellum, the major variables among strains of Cercomonadidae lie in the form and position of pseudopods, the number, size and position of contractile vacuoles, the thickness and texture of cyst walls, and the presence/absence of plasmodium and cysts in the life cycle. Our demonstration that certain strains of very different sequence can have a similar combination of light microscope characters means that in future it will be essential to combine an rRNA sequence with light microscope morphology of cultures in describing new species. Very few (e.g. *C. longicauda*, *C. alexeieffi,* C-43, and *N. plasmodialis* — Cs-4) of our strains can be identified with established species; we shall name additional new species elsewhere. We were agreeably surprised by the extent to which the molecular trees allow some patterns of phenotypic relationship of these remarkably pleomorphic amoeboflagellates to be discerned even in the light microscope. With sufficiently extensive sampling it should be possible to define species recognizable by a combination of morphology and rRNA signatures.

Although we have argued that Cercomonadidae are probably holophyletic, some recent trees suggest that this may not be true of the order Cercomonadida, currently comprising only Cercomonadidae and Heteromitidae (Cavalier-Smith and Chao 2003). The best and most comprehensive trees consistently place Heteromitidae closer to Thecofilosea and/or Imbricatea than to Cercomonadidae (Bass and Cavalier-Smith 2004; Bass et al. 2005). Although this has only weak support, if it were verified by other molecular analyses the two families may need separate orders. Cercomonadida were (weakly) holophyletic on only one of four trees of Cavalier-Smith and Chao (2003) and on none of those of Ekelund et al. (2004).

Ultrastructural Contrasts between *Cercomonas* (A1) and *Eocercomonas* (A2)

All 4 members of clade A1 (*Cercomonas*: C-84, C-59, RS/21 and C-43) have a general ultrastructure with slightly flattened tubular mitochondrial cristae, nuclear projection to centrioles, well-developed nucleolus, and extrusomes (osmiophilic bodies), whereas C-80 (clade A2: *Eocercomonas ramosa*) has no nuclear projection, extrusomes or nucleolus, but has prominent heterochromatin, developed ER around the central part of the cell including the nucleus, and tubular branching cristae. C-80 alone has branching filopodia in the amoeboid state. Centrioles also differ in these two clades: A1 has a thick distal partition with peripheral diaphragm-like structure and a cartwheel in the anterior centriole only; in A2 (C-80) both centrioles lack cartwheels, having a proximal transverse plate instead, and the distal partition is very thin with no peripheral diaphragm.

All four A1 strains have great similarity in root structure also (Table 2), but are rather different from C-80. A1 ventral posterior microtubules are organized as two distinct roots (VP2 and VP1), one attached to the side of the anterior centriole and the other embedded proximally in a dense sheet

Table 2. Morphological characteristics of cercomonads.

Characters	Strains												
	C-84, Rs/21, C-43, C-59 *Cercomonas* Clade A1 (present paper)	C-80 *Eocercomonas ramosa* Clade A2 (present paper)	C-52 (Mylnikov 1990)	Cs-9 *Paracercomonas metabolica* (Mylnikov, Mylnikova 2001, as *C. metabolicus*)	Cs-4 *Cercomonas plasmodialis* (Mylnikov et al. 2000)	C-1 (Mylnikov 1987)	C-57 (Mylnikov 1992b)	C-50 *activa* (Mylnikov, 1992a)	C-21 *varians* (Mylnikov 1986b)	C-45 (Mylnikov 1986c)	(Karpov 1997)	(Mignot, Brugerolle 1975)	(Schuster, Pollack 1978)
General ultrastructure													
ER around the nucleus	–	+	–	–	–	+	–	–	–	–	–	–	– ?
MRB	+	+	–	–	–	–	+	–	–	–	–	–	–
Mitochondrial cristae	tf	rt	tf	tf	ves	tf	ves	ves	tf	ves	tf	ves	ves
Extrusomes	ob	–	mtc	mtc	ob, tr	ob	–	ob, tr	ob	mtc	mtc, kc?	–	mtc
Nuclear projection to centrioles	+	–	+	+	+	+	+	+	+	+	+	+	+
Centriole characteristics													
Cartwheel structure	AC	–	AC, PC	AC	–	AC	AC	?	AC	AC, PC	AC, PC	AC, PC?	PC, AC?
Diaphragm	+	–	–	+	+	+	+	+	+	+	–	+	–
Transverse plate	–	+	+	–	+	–	+?	+	–	–	+	+	+?
Flagellar roots													
Root VP2	3—6	2—3											
Root VP1	4—7	4—5											
Left ant. root	2+smt	1											
sml	+	–											
sma	+	–											
Dorsal ant. root	2	1											
Dorsal post. root	–	+											
Nuclear fibrillar roots	2 branches from AC	1 str from AC	?	–	1str from AC	1 from AC	–	1 str	1 str	–?	1 str from AC	1 str from AC	+?
Microtubular cone	+	+	+	+	+	+	+	+	+	+	+	+	+

Numerals in flagellar roots section show the number of microtubules per root. Strains with no generic name have no available sequences. *Abbreviations*: "+" – present, "–"— absent, "?" — doubtful, AC— centriole of anterior flagellum, kc — kinetocysts, cs — centrioles, mtc—microtoxicysts, ob — osmiophilic bodies, PC — centriole of posterior flagellum, rt — rounded tubules, smt — secondary microtubules, str — striated fibrillar root, tf — tubular flattened, tr — trichocysts, ves — vesicular, MRB — mushroom-like bodies, sml — secondary microtubules from left root, sma — pair of microtubules from anterior centriole.

adjacent to the posterior centriole. These roots are in all investigated strains, but the number of microtubules is slightly different. VP2 normally starts as a 3-microtubule root, and VP1 as a 4—5-microtubule root. In all strains additional cytoplasmic microtubules broaden them to 5—7. Left and right strands of two microtubules accompany both roots.

In C-80 the VP2 has at its origin 2—3 (in different cells) and VP1 has 4—5 microtubules, both having almost no changes on their way backwards. A1 cercomonads have a well-developed microtubule-nucleating left anterior root, while in A2 it is much simpler without secondary microtubules. At the same time, it has an additional dorsal posterior root, absent in A1. C-80 has no striated spur from the anterior centriole, but its distinctive nuclear fibrillar root is striated, unlike the nuclear fibrillar roots of clade A1. The fewer microtubules associated with the posterior ventral roots (two distinct pairs totally absent) in C-80 may be the primitive state and its absence of secondary microtubules a derived state for Cercomonadidae as the heteromitid *Katabia* lacks the former but has the latter (Karpov et al. 2003a). Our preliminary serial sectioning study of one clade B strain shows that it is even more different from A1 than is A2, and relatively simple, suggesting that several distinctive characters of A1 are synapomorphies for it and not primitive characters of Cercomonadidae as a whole. We defer discussion of this until our clade B data are published.

Common Features of Clade A Flagella and Kinetids

Centrioles attach to each other obtusely or nearly orthogonally. In C-43, thin striation of the fibrillar main and broadest anterior bridge, connecting both centrioles, suggests its possible contraction and a flexibility of angle between the centrioles in life. If so, the angle might not be important for kinetid description in '*Cercomonas'*. More essential is the universal attachment of the posterior centriole to the surface of the anterior one at its approximate middle. Precisely this mode of attachment and approximately orthogonal centriolar orientation was found in all investigated '*Cercomonas*' (Karpov 1997; Mignot and Brugerolle 1975; Mylnikov 1986b, c 1987, 1989a, b, 1990, 1992a, b, 1995, 2000, 2001; Mylnikov and Mylnikova 2001; Mylnikov et al. 2000; Schuster and Pollack 1978): a very conservative character.

In all investigated strains five features of the root system are conserved: an association of two posterior ventral microtubular roots; left anterior root; dorsal anterior root; microtubular cone. The anterior centriole has two microtubular roots in clade A1 and three in clade A2. The posterior centriole has one microtubular root in all five strains. The left anterior root is common for both centrioles as it originates from their feet fusion, an important character found in *Katabia* and *Heteromita* also (Karpov et al. 2003a). Most roots pass to the left dorsal side of the cell, and the nuclear projection of A1 is from the left dorsal side of the centrioles, indicating a conserved geometry.

An ER cisterna was applied to root VP2 in all strains. A similar association of ER with centrioles is common in animals, choanoflagellates (Karpov and Leadbeater 1998) and some bicoecids (Karpov, unpublished); it might be present but overlooked in other Cercozoa and protists, and not distinctive for cercomonads. All strains had fibrillar roots to the nucleus, but their origin and composition are slightly different, and not conservative.

Comparison of our Strains with Other Investigated '*Cercomonas'* Species

Several strains were previously studied (Table 2), but none using serial sections, so detail was much less, and the origin, direction and exact location of the roots were not known. The main character previously noted in '*Cercomonas'* root systems was the microtubular cone — a set of single microtubules originating usually from the foot of the anterior centriole and directed to the nucleus (Karpov 1997; Mylnikov 1986a—c, 1987, 1989a, b, 1990, 1992a, b, 1995, 2000; Mylnikov and Mylnikova 2001; Mylnikov et al. 2000). It was accepted as a character of family Cercomonadidae, absent in Heteromitidae (Mylnikov and Karpov 2004). We found a cone in all investigated clade A strains, confirming its taxonomic significance. But the cone microtubules may originate from the anterior centriole (usually from its small posterior foot: clade A1a), from the base of the dorsal anterior root as secondary microtubules (C-80), or from the posterior centriole and fibrillar root, as in C-43. Some secondary microtubules from the left anterior root also pass to the nucleus. This emphasizes the ability of '*Cercomonas'* kinetids to extend microtubules towards the nucleus, possibly as spindle remnants after nuclear division.

One strain shown here to belong to clade A1 was studied previously: *C. plasmodialis* (Cs-4). It has a nuclear projection and obvious nucleolus, but has tubular non-flattened cristae and two kinds of extrusomes: trichocysts and osmiophilic bodies (Mylnikov et al. 2000, and our unpublished data). Our unpublished data show a distinctive nuclear striated root in Cs-4 even more prominent than in C-80, indicating that in some respects its morphological characters fit those reported here for clade A1, but it differs in a few, suggesting that ultrastructural diversity within *Cercomonas* (A1) may turn out to be even greater when more strains are studied thoroughly. A1 characters were present in '*C.' activas* (Mylnikov 1992a, Table 2). '*C'.* sp. (Mylnikov 1992b), had a distal centriolar diaphragm and nuclear projection, and thus may belong to clade A1.

Tubular flattened cristae were found in '*C.' varians* (Mylnikov 1986b), '*C. longicauda*' (Mylnikov 1987: there is no sequence evidence that this C-1 strain is related to either misidentified '*longicauda'* of clade B), and *P. metabolica* (Mylnikov and Mylnikova 2001). They also have a nuclear projection to the centrioles and the first two have osmiophilic bodies as extrusomes (Table 2). They could mostly belong to A1, but *P. metabolica* has microtoxicysts, not yet observed in A1. '*C.' varians* (Mylnikov 1986b) resembles A1 in most respects, but its striated nuclear root is an A2 character. Unlike in all other A1 strains, the cartwheel was not found in the anterior centriole of *C. plasmodialis* (Mylnikov et al. 2000); perhaps it was overlooked. A cartwheel was found in both centrioles of '*C.' cometa* (C-52: Mylnikov 1990) and '*C.'* sp. (C-57) (Table 2), suggesting that they may belong in clade B.

Reviews of '*Cercomonas'* transition zones embrace at least six species (Mylnikov 1995; Karpov and Fokin 1995). Most belong to a short type with one partition (transverse plate level with the plasma membrane), but some may have two partitions. '*C.' cometa* (Mylnikov 1990, 1995) has a distal centriolar diaphragm, unlike our C-80 *E. ramosa*, which has a very thin transverse plate. This ultrastructural difference and the different flagella lengths suggest that the original identification of C-80 as *C. cometa* was mistaken. By other characters '*C.' cometa* (strain C-52) is more similar to clade A1 than to clade A2 (Table 2). '*C.' activas* has two distal partitions: one corresponds with the transverse plate and another to the centriolar distal partition (Mylnikov 1992a, 1995). Concentric rings present in transitional regions of all members of clade A were found earlier in many cercomonads (Karpov and Fokin 1995; Mylnikov 1995; called a cylinder). As we do not know to which clade several of these species belong, we cannot deduce their evolutionary history. This emphasizes that all future ultrastructural studies of cercomonads should be on strains characterized by rRNA sequencing.

Centriolar Transformation in *Cercomonas*

An important conclusion of our study is that flagellar transformation occurs in Cercozoa and that the direction of transformation is from a younger anterior flagellum to an older posterior flagellum, as in all well-studied bikonts (Cavalier-Smith 2002). This follows from the fact that in all four clade A1 *Cercomonas* strains the posterior centriole is devoid of a cartwheel. Yet a cartwheel is present in both daughter centrioles, as in all eukaryotes. This means that later in development the cartwheel must be removed from the posterior centriole alone. The simplest interpretation of our evidence for the secondary removal of the cartwheel is that this is associated with flagellar transformation. We suggest that the anterior centriole and flagellum is transformed into the posterior centriole and flagellum in the next cell cycle after it is first assembled, as has been demonstrated to occur in many protists belonging to the plant and chromist kingdoms and to the protozoan infrakingdoms Alveolata and Excavata (Moestrup 2000). Our observations are the first evidence for centriole and flagellar transformation in any members of the protozoan infrakingdom Rhizaria. The pattern of transformation is from a young anterior to older posterior, precisely as predicted by Cavalier-Smith (2002) to be the ancestral state for all bikonts, not from a younger posterior to an older anterior as suggested by Moestrup (2000) by analogy with the mycetozoan *Physarum*.

Cercomonad Kinetids Differ Radically from those of Mycetozoa

Preliminary studies of kinetids of Cercomonadida were used to argue that Mycetozoa and Cercomonadida are related (Karpov 1997). This idea is not supported by molecular phylogeny and Cavalier-Smith (2002) argued in detail that the similarities between flagellar roots of Mycetozoa and *Cercomonas* on which the idea of a direct relationship between them was based are superficial. Our present study shows that *Cercomonas*

clade A does indeed have very different roots from Mycetozoa (compare with recent reconstructions of three myxogastrids: Karpov et al. 2003b). This confirms the overwhelming molecular evidence (Cavalier-Smith and Chao 2003) that Cercomonadida do not belong within Mycetozoa as has sometimes been suggested (Karpov 2000b). Previously flagellar transformation from a younger anterior to an older posterior flagellum was clearly demonstrated for many members of the plant kingdom, many chromalveolates and some excavates. Our demonstration that precisely the same pattern is present in Cercozoa, which belong to the only previously unstudied major group of eukaryotes, Rhizaria (Cavalier-Smith 2002), means that this pattern of flagellar transformation has now been found in all major bikont groups, as predicted (Cavalier-Smith 2002), and thus is indeed a synapomorphy for bikonts as a whole, being never found in unikonts such as Mycetozoa (see Cavalier-Smith et al. 2004). This strongly supports the idea that bikonts are a clade, in agreement with evidence that the root of the eukaryote tree lies between bikonts and unikonts (Cavalier-Smith 2002, 2003a, b; Richards and Cavalier-Smith 2005; Stechmann and Cavalier-Smith 2002, 2003a, b).

Comparisons with *Katabia* and other Bikonts

Reasonably convincing homologies can be drawn between the roots of *Cercomonas* and *Eocercomonas* and those of the heteromitid *Katabia* (Karpov et al. 2003a), even though *Katabia* (like *Heteromita globosa*) has no microtubular cone. The only *Katabia* root directly attached to the anterior centriole has two microtubules and appears positionally homologous to the 2-microtubule dorsal anterior root of clade A; it differs by being associated laterally with a fibrous band, and is thus a composite root (thus was labeled CR), not a simple root — we found a similar composite root in *Cercomonas* clade B (Karpov et al. in preparation), so the associated fibrous band may have been lost by the ancestor of clade A. Like clade A *Katabia* has a 2-microtubule left anterior root with secondary microtubules, starting also from fibrillar material associated with the anterior centriole, near to the feet fusion; we suggest that their left anterior roots may be homologues; that of *Katabia* was previously called the upper root (UR); the 2-microtubule posterior-pointing root called LR in *Katabia* lacks an obvious homologue in clade A cercomonads.

Katabia has a 'posterior band' of 4—5 microtubules originating from the dorsal side of both centrioles that passes under the plasma membrane alone to the posterior; this is arguably positionally homologous to cercomonad root VP2 (with three microtubules in A2 and proximally with three and distally with six microtubules in A1) as it initiates in almost the same place — beside rather than directly on the side of the anterior centriole. *Katabia* has a 'girdle root' of 3 microtubules stemming from the posterior centriole, which initially passes posteriorly beside the posterior band, then turns around the centrioles to the right side of the cell; the proximal association of the girdle and posterior bands is similar to that of roots VP1 and VP2 in C-80 (Fig. 13 M) and the girdle band stems from the same point on the posterior centriole as VP1. Since *Katabia*'s girdle band is also proximally ventral to the posterior band, as VP1 is to VP2, we suggest that these two roots are probably homologues, even though the distal path of the girdle band is much more divergent than for VP1, and that the characteristic proximal association of VP1 and VP2 on the left of the posterior centriole may be a synapomorphy for Sarcomonadea (heteromitids plus cercomonads). To test this and establish the ancestral state for Filosa, comparably detailed studies are needed for more divergent lineages, e.g. *Metopion* and *Metromonas*. There appear to be no cercomonad homologues of the 2-microtubule anterior band of the posterior centriole of *Katabia*. Thus four microtubular roots may be homologous between heteromitids and cercomonads. Information on *Heteromita globosa* (Macdonald et al. 1977) and *H*. sp. (Karpov 1997) is too limited for useful comparison: two posterior bands and a left anterior root were identified, but without more thorough study of *Heteromita* we cannot say whether it really lacks other roots identified in *Katabia*.

Our conclusion of four distinct conserved microtubular roots for sarcomonads is important for eventually reconstructing the ancestral bikont kinetid. Root VP1 may be positionally homologous with left root r1 of plants, chromalveolates, and excavates (Cavalier-Smith 2003b; Moestrup 2000; Simpson and Roger 2004), but in marked contrast to most of these other bikonts there appears to be no right posterior microtubular root (r2) in sarcomonads. Conversely, no obvious homologue of the sarcomonad root VP2 is present in other bikonts. Spongomonad cercozoans have only one microtubule band associated with each centriole, which might either be the ancestral state for all

Cercozoa (Cavalier-Smith 2002) or a secondary simplification. Kinetid structure must be determined from several more cercozoan classes before the ancestral state of Cercozoa, and then bikonts as a whole, can be reliably reconstructed.

Methods

Isolation and maintenance of cultures: The Mylnikov (Borok, Russia) cultures were isolated from these sites: Cs-4, C-56 and Cs-9 from soil (Borok, Russia), CeS-2 from freshwater lake (Germany), C-43 from sewage water (Russia), C-72 *Sphagnum* bog (Russia), C-85 from small pond (Borok, Russia), C-59 from freshwater lake C-71 and C-84 from river (Russia), C-76 and C-80 from a lake (Antarctica). *P. marina* was from ATCC ('*longicauda*' #50344). The Mylnikov strains were all clonal cultures made by isolating single cells by a glass micropipette, and maintained in Petri dishes on artificial Pratt medium (KNO_3 0.1‰, $K_2HPO_4 \cdot 3H_2O$ 0.01‰, $MgSO_4 \cdot 7H_2O$ 0.01‰, $FeCl_3 \cdot 6H_2O$ 0.001‰; pH 6.5—7.5) with the addition of bacteria *Klebsiella aerogenes* or wheat grains as the source of food at 20—22 °C. The Bass (Oxford) strains were isolated from crude soil and freshwater samples immediately after collection by serial dilution into a 96-well cell culture plate (Nunclon). Volvic mineral water (Danone) was added to soil samples immediately after collection, without flooding them, to facilitate pipetting after a period of incubation at room temperature for approximately 1 week. Serial dilution was achieved by inoculating 250 μl of medium (ca. 150 ml Volvic water which had previously been boiled in the microwave for 3 min with ca. 20 grains of untreated wheat or barley; subsequently maintained at 4 °C) with 50—100 μl of crude culture. This was mixed by repeatedly pipetting up and down; then the same volume as the inocculant was transferred to a second well containing 250 μl fresh medium. This manoeuvre was repeated 7 times for each strain. The 96-well plate was sealed with parafilm and left at room temperature to incubate for 1—2 weeks. The wells were then examined and cultures grown from those wells containing only '*Cercomonas*' and bacteria. The serial dilution procedure was repeated in cases where the final well contained other eukaryotes as well as '*Cercomonas*'. Stock cultures are maintained at 14 °C in the same medium, including the cereal grain, and subcultured ideally at 3-monthly intervals. Cultures are available from the authors upon request.

Light microscopy: Light microscopy on living material in Russia used the Biolam-I (Russia) microscope equipped with a video camera MC-1009/S (Germany) and phase contrast water immersion 70 × objective (KF-5 device, Russia). Development of the cultures was recorded by a Panasonic NV-HS850 (Japan) video recorder. The videotape recording was digitized by PC computer and saved in formats such as *avi*, *tiff*. The Oxford strains were photographed using a × 40 dry phase contrast lens on an inverted Olympus IX70 microscope equipped with a Nikon Coolpix 995 digital camera. Digital (.jpeg) images were transferred to Photoshop v.5.5 (Adobe) for processing.

DNA purification, sequencing, phylogenetic analysis: Cultures were harvested after reaching stationary growth phase by gently scraping the bottom of the culture dish with a sterile scraper, and concentrating the cells by one of two methods: filtering under low pressure through a glass-fibre filter (Whatman GF/F) which was cut into small pieces before the first (homogenization) step, or centrifuging the liquid culture at 2,000 rpm in a benchtop centrifuge for 10—15 min at 5 °C, then pipetting out the pellet of organic material. Total DNA was extracted using the UltraClean Soil DNA Isolation Kit (Mo Bio Laboratories), subjecting either the finely chopped filter or 200 μl of medium with organic pellet to the first (homogenization) step or directly from 1 g soil samples. 18S rRNA gene sequences were amplified by PCR with one or two of three primer pairs: (1) the '*Cercomonas*' Clade A-specific 243F (5′-CCA-ATGCACCCTCTGGGTGGTT-3′) and the '*Cercomonas*' Clade A-biased 1733R (5′-TGATCAA-GTTTGATTCAGTTCTCGGAT-3'); (2) 25F (5′-CAT-ATGCTTGTCTCAAAGATTAAGCCA-3′) and the cercozoan-specific 1256R (5′-GCACCACCACC-CAYAGAATCAAGAAAGAWCTTC-3′); (3) the Cercozoa-specific 1259F 5′-GGT CCR GAC AYA GTR AGG ATT GAC AGA TTG AAG-3′ and general eukaryote 369R 5′-TCG CAT TAC GTA TCG CAT TTC GCT G-3′ under cycling conditions: 5 min at 95 °C, 30 cycles of (32 s at 95 °C, 36 s at 70 °C, and 3 min 30 s at 72 °C), then 8 min at 72 °C. The products were run on a 1% agarose gel. Bands of correct length were excised, cleaned using a GFX PCR DNA Gel Band Purification Kit (Amersham Biosciences), sequenced using dye terminators and separated on an automated ABI-377 sequencer. Sequencing primers were the initial PCR primers and an internal primer Pre3NDf (5′-CAGCAGGCGCGCAAATTACC-3′). Complete sequences were obtained from cultures but only

partial ones from soil samples. Sequences were edited in the trace editor TED and deposited in GenBank under accession numbers AY884312—AY884342 and DQ442884.

Sequences were aligned by eye with all existing '*Cercomonas*' sequences in our database using Genetic Data Environment software. These sequences included those from other cultures and from environmental libraries constructed using Cercozoa-specific primers (Bass and Cavalier-Smith 2004). Gaps and ambiguously aligned positions were removed, leaving 1013 positions across 56 sequences, including the five heteromitid outgroups. ModelTest v.3.06 (Posada and Crandall 1998) selected the GTR model with gamma correction for intersite rate variation (Γ; $\alpha = 0.524154$) and allowance for invariant sites ($i = 0.330625$). These parameters were used for distance trees constructed using PAUP 4.0b10 (Swofford 1999). Heuristic searches (1000 replicates with no time limit per replicate; random addition) using minimum evolution were made (with TBR branch swapping). Bootstrap support values were estimated using 500 bootstrap replicates for each of 50 addition sequence replicates for a distance analysis using the same GTR+Γ+I model. Sequence alignments are available on request from DB.

The Bayesian tree (Fig. 1) was calculated using MrBayes v3.0b4 (Huelsenbeck and Ronquist 2001) based on 56 taxa and 1013 positions. Two separate MCMC runs with randomly generated starting trees were carried out for 3 million generations each with one cold and three heated chains. The evolutionary model applied included GTR substitution matrix, gamma correction with shape parameter estimated from the data, the covarion model, and autocorrelation. Trees were sampled every 100 generations. A total of 5500 trees were discarded as burn-in (trees sampled before the likelihood plots reached a plateau). A consensus of the remaining trees was generated to reveal posterior probabilities of the branching pattern. Both independent runs resulted in basically identical tree topologies and posterior probabilities, indicating that they lasted long enough to converge.

Electron microscopy: Cells were fixed with a fresh mixture of 0.6% osmium tetroxide with 1.4% glutaraldehyde (2 ml fixative (1 ml 2% of osmium tetroxide+1 ml of 4.25% glutaraldehyde)+1 ml of cells in medium) in 0.05 M phosphate buffer pH 7.3 (final concentrations) at 0 °C in the dark for 30—40 min. After dehydration in an alcohol series and acetone, the pellet was embedded in Araldite. Blocks were serially sectioned with a diamond knife on a Reichert ultramicrotome, mounted on formvar-coated slot grids, and post-stained with uranyl acetate and lead citrate. Sections were viewed on a JEM 100CX electron microscope operating at 80 kV. For three-dimensional reconstruction of kinetid patterns, serial sections of the flagellar apparatus of at least 10 cells of each species were examined. To exclude potential mistakes with rootlet interpretation, we did not analyse micrographs of predivision stages, when additional centrioles appear; just prior to mitosis, additional roots appear in conjunction with centriole duplication.

Note added in proof

The newly described cercozoan *Aurigamonas* also exhibits transformation from young anterior to old posterior flagellum (Vickerman et al. 2005).

Acknowledgements

The work was supported by a NERC research grant and Professorial Fellowship to TC-S and studentship to DB, by RFBR grants 02-04-49987 and 02-04-48265 to APM and SAK, and a joint project grant from the Royal Society. TC-S thanks the Canadian Institute for Advanced Research Evolutionary Biology Programme for Fellowship support and Ema Chao for assistance.

References

Al-Qassab S, Lee WJ, Murray S, Simpson AGB, Patterson DJ (2002) Flagellates from stromatolites and surrounding sediments in Shark Bay, Western Australia. Acta Protozool **41**: 91—144

Arndt H, Dietrich D, Auer B, Cleven E-J, Gräfenham T, Weitere M, Mylnikov AP (2000) Functional Diversity in Aquatic Ecosystems. In Leadbeater BS, Green JC (eds) The Flagellates: Unity and Diversity. Taylor & Francis, London, pp 240—268

Archibald JM, Longet D, Pawlowski J, Keeling PJ (2003) A novel polyubiquitin structure in Cercozoa and foraminifera: evidence for a new eukaryotic supergroup. Mol Biol Evol **20**: 62—66

Bass D, Cavalier-Smith T (2004) Phylum-specific environmental DNA analysis reveals remarkably high global biodiversity of Cercozoa (Protozoa). Int J Syst Evol Microbiol **54**: 2393—2404

Bass D, Moreira D, López-García P, Polet S, Chao EE, von der Heyden S, Pawlowski J, Cavalier-Smith T (2005) Polyubiquitin insertions and the phylogeny of Cercozoa and Rhizaria. Protist **156**: 149—161

Cavalier-Smith T (1974) Basal body and flagellar development during the vegetative cell cycle and the sexual cycle of *Chlamydomonas reinhardii*. J Cell Sci **16**: 529—556

Cavalier-Smith T (1998) A revised six-kingdom system of life. Biol Rev Cambridge Philos Soc **73**: 203—266

Cavalier-Smith T (2002) The phagotrophic origin of eukaryotes and phylogenetic classification of Protozoa. Int J Syst Evol Microbiol **52**: 297—354

Cavalier-Smith T (2003a) The excavate protozoan phyla Metamonada Grassé emend. (Anaeromonadea, Parabasalia, *Carpediemonas*, Eopharyngia) and Loukozoa emend. (Jakobea, *Malawimonas*): their evolutionary affinities and new higher taxa. Int J Syst Evol Microbiol **53**: 1741—1758

Cavalier-Smith T (2003b) Protist phylogeny and the high-level classification of Protozoa. Europ J Protistol **39**: 338—348

Cavalier-Smith T, Chao EE (1996/7) Sarcomonad ribosomal RNA sequences, rhizopod phylogeny, and the origin of euglyphid amoebae. Arch Protistenkd **147**: 227—236

Cavalier-Smith T, Chao EE (2003) Phylogeny and classification of phylum Cercozoa (Protozoa). Protist **154**: 341—358

Cavalier-Smith T, Chao EE (2006) Phylogeny and megasystematics of phagotrophic heterokonts (kingdom Chromista). J Mol Evol **62**: 388—420

Cavalier-Smith T, Chao EE, Oates B (2004) Molecular phylogeny of Amoebozoa and the evolutionary significance of the unikont *Phalansterium*. Europ J Protistol **40**: 21—48

Dujardin F (1841) Histoire Naturelle des Zoophytes Infusoires. Roret, Paris

Ekelund F, Patterson DJ (1997) Some heterotrophic flagellates from a cultivated soil in Australia. Arch Protistenkd **148**: 461—478

Ekelund F, Daugbjerg N, Fredslund L (2004) Phylogeny of *Heteromita*, *Cercomonas* and *Thaumatomonas* based on SSU rDNA sequences, including the description of *Neocercomonas jutlandica* sp. nov., gen. nov. Europ J Protistol **40**: 119—135

Finlay BJ (2002) Global dispersal of free-living microbial eukaryote species. Science **296**: 1061—1063

Finlay BJ, Clarke KJ (1999) Apparent global ubiquity of species in the protist genus *Paraphysomonas*. Protist **150**: 419—430

Foissner W (1991) Diversity and Ecology of Soil Flagellates. In Patterson DJ, Larsen J (eds) The Biology of Free-Living Heterotrophic Flagellates. Clarendon Press, Oxford, pp 93—112

Fromentel FDE (1874) Études sur les Microzoaires ou Infusoires Proprement dit. Masson, Paris

Hollande A (1942) Etude Cytologique et Biologique de Quelques Flagellés Libres. Arch Zool exp générale **83**: 1—268

Huelsenbeck JP, Ronquist F (2001) MRBAYES: Bayesian inference of phylogenetic trees. Bioinformatics **17**: 754—755

Karpov SA (1997) Cercomonads and their relationship to myxomycetes. Arch Protistenkd **158**: 297—307

Karpov SA (2000a) Flagellate Phylogeny: an Ultrastructural Approach. In Leadbeater BSC, Green JC (eds) The Flagellates: Unity, Diversity and Evolution. Taylor & Francis, London, pp 336—360

Karpov SA (ed) (2000b) Protista: Handbook on Zoology Pt 1. Nauka, St. Petersburg

Karpov SA, Fokin SI (1995) The structural diversity of flagellar transitional zone in heterotrophic flagellates and other protists. Tsitologia **37**: 1038—1052

Karpov SA, Ekelund F, Moestrup Ø (2003a) *Katabia gromovi* nov. gen., nov. sp. — a new soil flagellate with affinities to *Heteromita* (Cercomonadida). Protistology **3**: 30—41

Karpov SA, Novozhilov YK, Christiakova LV (2003b) A comparative study of zoospore cytoskeleton in *Symphytocarpus impexus*, *Arcyria cinerea* and *Lycogala epidendrum* (Eumycetozoa). Protistology **3**: 15—29

Keeling PJ (2001) Foraminifera and Cercozoa are related in actin phylogeny: two orphans find a home? Mol Biol Evol **18**: 1551—1557

Kent WS (1880—1882) A Manual of the Infusoria. Bogue, London

Klebs G (1892) Flagellatenstudien. Zeit wiss Zool **55**: 265—445

Krassilstschik I (1886) The materials to the natural history and taxonomy of flagellates. On *Cercobodo laciniaegerens* nov. gen. et nov. sp. Zapiski Novosibirskogoobschestva estestvoispytatelei. **2**, 1, 211—245 (in Russian)

Lee WJ, Patterson DJ (2000) Heterotrophic flagellates (Protista) from marine sediments of Botany Bay, Australia. J Nat History **34**: 483—562

Lemmermann E (1914) Flagellatae 1. Gustav Fischer, Jena

Macdonald CM, Darbyshire JF, Ogden CG (1977) The morphology of a common soil zooflagellate, *Heteromita globosa* Stein (Mastigophorea: Protozoa). Bull Br Mus Nat Hist (Zool) **31**: 255—264 + 6 plates

Mignot J-P, Brugerolle G (1975) Étude ultrastructurale de *Cercomonas* Dujardin (= *Cercobodo* Krassilstchick) protiste flagellé. Protistologica **11**: 547—554

Moestrup Ø (2000) The Flagellate Cytoskeleton: Introduction of a General Terminology for Microtubular Roots in Protists. In Leadbeater BS, Green JC (eds) The Flagellates: Unity, Diversity and Evolution. Taylor & Francis, London, pp 69—94

Mylnikov AP (1986a) The biology and ultrastructure of amoeboid flagellates Cercomonadida ord. n. Zoologicheskii Zhurnal, Moscow **65**: 683—692 (in Russian with English summary)

Mylnikov AP (1986b) The peculiarities of ultrastructure *Cercomonas varians*. Tsitologiya **28**: 414—417 (in Russian with English summary)

Mylnikov AP (1986c) Ultrastructure of a colourless amoeboid flagellate, *Cercomonas* sp. Arch Protistenkd **131**: 239—247

Mylnikov AP (1987) The ultrastructure of flagellate *Cercomonas longicauda* (Cercomonadida) Bot Zhurn **72**: 750—753 (in Russian with English summary)

Mylnikov AP (1989a) The cell structure of flagellate *Cercomonas crassicauda*. Biologia vnutrenih vod Inform bul **84**: 22—26 (in Russian)

Mylnikov AP (1989b) The rootlet flagellar system of cercomonads. Biologia vnutrenih vod Inform bul **84**: 52—54 (in Russian)

Mylnikov AP (1990) The cell structure of flagellate *Cercobodo cometa*. Biologia vnutrenih vod Inform bul **86**: 33—38 (in Russian)

Mylnikov AP (1992a) The cell structure of the flagellate *Cercomonas activus*. Biologia vnutrenih vod Inform bul N **92**: 14—19 (in Russian)

Mylnikov AP (1992b) The structure of amoeboid flagellate *Cercomonas sp*. Biologia vnutrenih vod Inform bul N **94**: 41—45 (in Russian)

Mylnikov AP (1992c) Some taxonomic features of cercomonads. Biologia vnutrenih vod Inform bul **93**: 35—39 (in Russian)

Mylnikov AP (1995). The Free-Living Heterotrophic Flagellates (Ultrastructure, Systematics and Biology). DSc Thesis. St. Petersburg: St. Petersburg State University (in Russian)

Mylnikov AP (2000). Class Cercomonadea Mylnikov, 1986 — Cercomonads. In Alimov AF, Stepanjantz SD, Karpov SA (eds) Protista, I: Handbook on Zoology. Nauka, St. Petersburg. pp 411—417 (in Russian with English summary)

Mylnikov AP (2002) New amoeboid flagellates of the genus *Cercomonas* (Cercomonadida, Protozoa) from lakes of Spitzbergen island. Zoologicheski Zhurnal Moscow **81**: 1187—1192 (in Russian with English summary)

Mylnikov AP, Mylnikova ZM, Tsvetkov AI (2000) The fine structure of amoeboid flagellate *Cercomonas plasmodialis* Mylnikov. Biologia vnutrenih vod N **4**: 29—35 (in Russian with English summary)

Mylnikov AP, Mylnikova ZM (2001) The main ultrastructure of amoeboid flagellate *Cercomonas metabolicus* Mylnikov, 1987. Biologiya Vnutrenih Vod N **2**: 65—69 (in Russian with English summary)

Mylnikov AP, Karpov SA (2004) Review of the diversity and taxonomy of cercomonads. Protistology **3**: 201—217

Nikolaev SI, Berney C, Fahrni JF, Bolivar I, Polet S, Mylnikov AP, Aleshin VV, Petrov NB, Pawlowski J (2004) The twilight of Heliozoa and rise of Rhizaria, an emerging supergroup of amoeboid eukaryotes. Proc Natl Acad Sci USA **101**: 8066—8071

Polet S, Berney C, Fahrni J, Pawlowski J (2004) Small-subunit ribosomal RNA gene sequences of Phaeodarea challenge the monophyly of Haeckel's Radiolaria. Protist **155**: 53—63

Posada D, Crandall KA (1998) MODELTEST: testing the model of DNA substitution. Bioinformatics **14**: 817—818

Richards TA, Cavalier-Smith T (2005) Myosin domain evolution and the primary divergence of eukaryotes. Nature **436**: 1113—1118

Sandon H (1927) The Composition and Distribution of the Protozoan Fauna of the Soil. Oliver & Boyd, Edinburgh

Schuster FL, Pollack A (1978) Ultrastructure of *Cercomonas* sp., a free-living amoeboid flagellate. Arch Protistenkd **120**: 206—212

Simpson AGB, Roger AJ (2004) Excavata and the Origin of Amitochondriate Eukaryotes. In Hirt RP, Horner DS (eds) Organelles, Genomes, and Eukaryote Phylogeny, The Systematics Association

Special Volume Series 68. CRC Press, Boca Raton, Florida, pp 27—33

Skvortzov BV (1977) The flagellates of clear and polluted waters. New taxa of the genus *Cercobodo* Krassil: a colourless flagellate of Rhizomastigaceae, Pantostomatinae. Q J Taiwan Mus Taipei **30**: 89—121

Stechmann A, Cavalier-Smith T (2002) Rooting the eukaryote tree by using a derived gene fusion. Science **297**: 89—91

Stechmann A, Cavalier Smith T (2003a) The root of the eukaryote tree pinpointed. Curr Biol **13**: R665—R666

Stechmann A, Cavalier-Smith T (2003b) Phylogenetic analysis of eukaryotes using heat-shock protein Hsp90. J Mol Evol **57**: 408—419

Stein FR (1878) Der Organismus der Infusionsthiere, III: Der Organismus der Flagellaten I. Engelmann, Leipzig

Swofford DW (1999) PAUP* 4.0b10. Sinauer, Sunderland, MS

Vickerman K, Appleton PL, Clarke KJ, Moreira D (2005) *Aurigamonas solis* n. gen., n. sp., a soil-dwelling predator with unusual helioflagellate organisation and belonging to a novel clade within the Cercozoa. Protist **156**: 335—354

von der Heyden S, Cavalier-Smith T (2005) Culturing and environmental DNA sequencing uncover hidden kinetoplastid biodiversity and a major marine clade within ancestrally freshwater *Neobodo designis*. Int J Syst Evol Microbiol **55**: 2605—2621

Wuyts J, De Rijk P, Van de Peer Y, Pison G, Rousseeuw P, De Wachter R (2000) Comparative analysis of more than 3000 sequences reveals the existence of two pseudoknots in area V4 of eukaryotic small subunit ribosomal RNA. Nucleic Acids Res **28**: 4698—4708

Zhukov BF (1993) Atlas of Freshwater Heterotrophic Flagellates. Russian Academy of Sciences, Institute of the Biology of Inland Waters, Rubinsk (in Russian)